GLOBAL SCALE BEDLOAD FLUX MODELING

by

MD TAZMUL ISLAM

SAGY COHEN, COMMITTEE CHAIR
SARAH PRASKIEVICZ
MARK ELLIOTT

A THESIS

Submitted in partial fulfillment of the requirements
for the degree of Master of Science
in the Department of Geography
in the Graduate School of
The University of Alabama

TUSCALOOSA, ALABAMA

2018

ABSTRACT

Bedload flux is an important component of the total fluvial sediment flux. Bedload dynamics can have a substantial effect on rivers and coastal morphology, infrastructure sustainability, aquatic ecology and water availability. Bedload measurements, especially for large rivers, are extremely scarce worldwide, where most global rivers have never been monitored. The paucity of bedload measurements is the result of 1) the nature of the problem (large spatial and temporal uncertainties), and 2) high costs due to the time-consuming nature of the measurement procedures (repeated bedform migration tracking, bedload samplers). Numerical models can help fill measurement gaps and provide a framework for predictions and hypothesis testing. Here, I present a first of its kind global bedload flux model using simplified Bagnold Equation, which considers only two dynamic (discharge and river slope) parameters along with few constant parameters (e.g., gravity, sediment density). Evaluation of model has been done based on observations for 59 river locations, mostly in the U.S. The model parameters, as well as other influential fluvial and basin parameters (e.g., discharge, drainage area, lithology), were evaluated against observed bedload to find their potential influence on bedload prediction. Considering the simplicity in the parameters needed to predict bedload flux through this model, and the capabilities to give first order estimation the model is helpful to give the large-scale overview of dynamic bedload flux universally. Also, the longitudinal dynamics between suspended and bedload sediment fluxes are mapped in three large rivers.

DEDICATION

This research is dedicated to my parents for encouraging me to pursue higher studies, and to be always on my side.

LIST OF ABBREVIATIONS AND SYMBOLS

DEM	Digital Elevation Model
HydroSHEDS	Hydro SHuttle Elevation Derivatives
WBMsed	Water Balance Model (sediment)
Qb	daily bedload flux
Qi	Daily mean water discharge
ρs	sediment density
ρ	fluid density
e_b	Bedload efficiency
λ	limiting angle of repose of sediment grains lying on the river bed
GPCC	Global Precipitation Climate Center
NCEP	National Centers for Environmental Predictions

ACKNOWLEDGMENTS

First, I would like to pay my gratitude to my advisor Dr. Sagy Cohen, for his continuous guidance, and excellent mentorship throughout my Master's degree. All the support, and instructions that I got from him makes it possible to finish my research successfully.. Thanks to my committee member Dr. Sarah Praskievicz, and Dr. Mark Elliott for their advice and suggestions.

I would also like to acknowledge for all the support, and company of my lab mates Dinuke, Mariam, Nishani, James, Brad. Their companionship helped to feel like home this whole time. Without their companion this would have been a difficult journey.

I would also like to acknowledge National Science Foundation for funding me for this research (Award Number 1561082).

Lastly, I am indebted to parents for supporting and understanding me during this time periods. Their inspiration helps me to come this far, and hope to continue this journey in future.

CONTENTS

LIST OF TABLES

LIST OF FIGURES

LIST OF EQUATIONS

CHAPTER 1

INTRODUCTION

Sediments movement along the stream bed by rolling, sliding or saltation, referred to as bedload flux (Habibi and Sivakumar 1994; Turowski et al. 2010; Wang et al. 2011, Emmett, 1984; Leopold and Emmett, 1976), is a key morphodynamic process (Lajeunesse et al., 2010), controlling the form and function of river systems (Habersack and Laronne 2002; Barry et al. 2008). Quantifying bedload transport has long been an area of interest for both scientists and engineers in the fields of geomorphology, hydraulic engineering, and management of rivers, estuaries, and coastal waters (Rickenmann et al., 2012). Better prediction of bedload flux is essential for proper management of fluvial aquatics, for navigation purpose, during dam construction, for flood defense, to maintain marine ecology, for food security, and for many other fluvial and coastal dynamics. Despite of over 100 years of research, the ability to robustly measure and predict bedload transport remains challenging due to its dynamic and complex nature (Gomez and Church, 1989, Lajeunesse et al., 2010).

Bedload can represent a significant fraction of total sediments transported within rivers (up to 60%), especially for headwater rivers (Métivier et al., 2004; Meunier et al., 2006; Liu et al., 2008). Globally, bedload contributes about 10 percent of total river sediment that is transported to the oceans (Meade et al., 1990). Turowski et al. (2010) found from their compiled

sediment datasets that bedload varies from 1 to 50 percent of total river sediment budget, and it can be even more influential for ephemeral rivers. Due to this dynamic nature, a large-scale perspective of bedload dynamics is needed to develop more universal insights into the spatial and temporal functioning of bedload transport across and within river basins.

Despite its importance, observational bedload data is scarce worldwide (Leopold and Emmett, 1976, 1997; Gomez and Church, 1989; Gomez, 1991, 2006; Ryan and Emmett, 2002; King et al., 2004), particularly for large rivers. The scarcity of bedload data is particularly acute in developing countries where changes in sediment yields are usually high (Walling and Fang, 2003). The main reasons for lack of observational data are the complex, labor-intensive, and costly measurement procedures for bedload (Turowski et al., 2010). Some bedload data is available thanks to observations made by different organizations (e.g., U.S. Geological Survey, U.S. Army Corps of Engineers, U.S. Forest Service), and individual researchers, primarily in the U.S. (Thaxton, 2004).

Although, bedload flux measurement through bedload traps/samplers is a standard procedure, it is difficult to extrapolate these point observations due to the high spatial and temporal variability even during steady flow conditions caused by bed roughness and irregularities in bed topography (Garcia et. Al., 2000). Due to these uncertainties in bedload measurement, and limitations in data availability, bedload flux data is often estimated as a fraction of measured suspended load (Syvitski and Saito, 2007), which led to biased results in most of the cases. Since spatially and temporally dynamic bedload transport rate cannot be obtained solely based on in situ measurements, the possibility of numerically estimating bedload flux is attractive (Habersack and Laronne, 2002). Different field sampling and laboratory

experiment allowed fluvial geomorphologists to develop bedload equations and models, significantly improving our understanding of bedload flux dynamics. Various formulas were derived based on different hydraulic conditions, and for different grain sizes. Flume experimental data has been widely used for developing a variety of bedload formulas (e.g., Gilbert, 1914; USWES, 1935; Shields, 1936; Chang, 1939; and Hamamori, 1962), while a few formulas have been developed based on field measurements (e.g., Schoklitsch, 1950; Rottner, 1959; Parker et al., 1982; Bathurst, 2007).

Many empirical and physically-based equations and models have been developed over the centuries for estimating bedload transport (e.g., Shields, 1936; Einstein, 1944; Meyer-Peter and Muller, 1948; Bagnold, 1966; Paola, 1996). Lechalas (1871) and Du Boys (1879) pioneered the development of bedload transport formulas, which provides the baseline for later work. With more data becoming available after 1900, some equations have been calibrated and applied during the 20th century. According to Reid et al. (1996) and Martin (2003) the Meyer-Peter and Muller (1948), Bagnold (1980) and Parker (1990) formulas are prime examples of these quantitative advances.

The Meyer-Peter and Muller (MPM) (1948) formula was designed for well sorted fine gravel (Whipple, 2004). MPM was developed based on 16-year experiments conducted at the Swiss Federal Institute of Technology in Zurich, Switzerland, with uniform 5.05 mm and 28.6 mm gravels, incorporating velocity relationships. This relationship has been modified in the MPM equation and allows bedload flux estimation in open-channels. The MPM equation is mainly used to deal with the relationship between shear stress and volumetric sediment discharge per unit width.

Gomez and Church (1989) tested twelve bedload transport formulas with four sets of river data and three sets of flume data for gravel bed channels. They considered particles coarser than 0.2 mm as bedload because the Halley-Smith sampler used for bedload data collection can only efficiently sample particles coarser than 0.2 mm. From their test of the twelve bedload equations with 358 field sample measurements they concluded that none of the bedload equations performed consistently well for bedload predictions, but suggested that with limited hydraulic information, the stream power equation (e.g., Bagnold, 1980) should be used for finding bedload transport due to the most straightforward correlation of the phenomena. Gomez and Church (1989) found that most of the formulas over-predicted bedload transport and suggested that formula calibration can reduce the bias between observed and predicted values. As they found Bagnold (1980) as one of the best formulae from its predictive performance for bedload, they recommended it for further study, noting that the formula over-predicted bedload transport in some cases.

Almadeij and Diplas (2003) used 174 field observations to study bedload transport with four equations and concluded that none of the equations performed consistently well because of over- or under-predictions. Bravo-Espinosa et al. (2003) used 1020 bedload observations in 22 gravel bed streams to test the predictability of 7 different bedload equations. From the results of the study, they concluded that the MPM model provided a reasonable estimation of bedload transport in limited situations, yet still performed better than other bedload equations. Martin (2003) conducted ten years of a survey on the Vedder River, British Columbia to test the performance of the MPM equation and two variants of the Bagnold (1980) equation and concluded that both formulas generally under predict gravel transport rate.

Barry (2004) used 2140 bedload transport observations for 24 gravel bed rivers in Idaho and concluded that the accuracy of predicted bedload transport rates depends on what equation has been used in what conditions. Khorram and Ergil (2010) studied around 300 important parameters for 52 selected bedload equations, for both sand and gravel bed separately. They suggested calculating bedload flux with great caution due to its complex and empirical or semi-empirical nature. They also concluded that sediment flux is a complex phenomenon and it might not be possible to express through a deterministic mathematical framework. Kabir et al. (2012) also applied different bedload equations at the Abukuma River Basin, Japan to find the appropriate bedload equation for accurate bedload estimation and concluded that the equations they used were not able to estimate bedload accurately.

Despite the reputation of many of these models and equations, there were some limitations for their applicability. There has been uncertainty among researchers with different equations and approaches, as each equation is developed based on parameters that differ from one another, and each parameter has its own range of validity and applicability (Zhang and McConnachie, 1994; Martin, 2003; Sinnakaudan et al., 2006). These include difficulties in quantifying or calibrating some of the key variables which limit the ability to generalize the equations or models to regions with various climatic, topographic and geologic conditions (Raven et al., 2010; Abrahart and White, 2001) and hinders global scale analysis.

Bagnold (1966) developed an earlier version of a simple bedload transport formula which shows a close correlation of bedload transport rate for both laboratory data and in a wide variety of natural rivers. He found that the bedload transport rate varies with grain size, and flow depth (e.g., bimodal bed material shows a random transport rate). The Bagnold (1966) equation is relatively robust for large-scale applications because it was derived based on the data for a wide

variety of natural rivers, and for experimental data as well. The Bagnold (1966) equation seemed suitable for global-scale modeling and is proposed here as the governing equation because the parameters of this equation can easily be approximated at different scales. Moreover it is arguably ideal for large rivers compared to the other bedload equations given the very high uncertainty associated with the previously described formulae. Syvitski and Saito (2007) introduced a modified version of the Bagnold (1966) equation to calculate the average and maximum bedload flux at 51 global river deltas. The modified Bagnold equation (1966), consider only two dynamic parameters (discharge and river slope), which are relatively easy to get globally. Considering the complex and large number of parameters (e.g., grain size, shear stress) used to predict bedload flux which is not available at global scale, they argued that using the modified Bagnold (1966) equation is reasonable. This modified Bagnold equation has been incorporated into HydroTrend v.3.0 model by Kettner and Syvitski (2008) to simulate daily bedload flux, and is used in this research to simulate daily bedload flux globally.

Numerical models can fill the gaps in sediment measurements (e.g., Syvitski et al., 2005), and offer predictive or analytical capabilities of future and past trends enabling the investigations of terrestrial response to environmental and human changes (e.g., climate change; Kettner and Syvitski, 2009). Using past trends is the best strategy for developing these (spatially and temporally explicit) models and improving our understanding of the dynamics and causality within these complex systems (Cohen et al., 2014). Cohen et al. (2013) developed the WBMsed model, a numerical model for suspended sediment transport calculation. This model works as a bridge to fill gaps in global sediment data. The WBMsed model is a spatially and temporally explicit (pixel-scale and daily) sediment model implemented based on the BQART model (Syvitski and Miliman, 2007). This model has been tested with observed sediment flux data from

95 rivers and 11 years of sediment observations from 11 USGS stations. This model includes many of the desired inputs are essential for developing a bedload flux model, and this modeling framework has been used for this research to establish a global bedload flux model.

Here I introduce the first global-scale bedload flux model. The overall goal of this research is to advance our understanding of riverine bedload flux dynamics at a global extent through the development of a spatially and temporally explicit global bedload flux model to get a good first order of estimation. A comprehensive observational database of bedload (particularly for large rivers >1000 km^2) has been compiled as part of this study from different sources (reports, websites). The first goal of this research is the evaluation of the universal applicability of the proposed model of bedload flux (the modified Bagnold (1966) equation). The model predictions have been evaluated against the observational bedload dataset (see: data collection section). Moreover, the relationships between bedload flux, and fluvial and basin parameters (e.g., discharge, drainage area, lithology, slope, etc.) have also been explored and tested.

There are two hypotheses of this study. First, it is hypothesized that the model will provide a good first-order estimation of bedload transport, compared to complex multi-variable bedload equation. Dozens of equations were developed over the years based on complex, multi-variables scenarios, but this simple Bagnold (1966) equation based bedload model would be good enough to simulate larger dynamics in the field of fluvial geomorphology and sediment dynamics. The model aims to get only first order of estimation, because of the lacking within the simulation framework to consider anthropogenic (dams, land use) impact on bedload. The second hypothesis is that the ratio between suspended sediment and bedload along rivers is driven by basin characteristics. Conceptually, the percent of sediment transported in suspension increases downstream, with bedload dominating steep headwater streams, and suspended flux

dominating (~90%) coastal rivers. Focusing on large rivers (basin area >1,000 km^2), it is hypothesized for this study that suspended to bedload ratio will show quantifiable and universal trends and that their ratio is dominated by basin characteristics (e.g. geology, hydrology). So, after completion of the development of the global bedload flux model, the spatial changes between suspended sediment and bedload was analyzed in different large rivers, and the factors responsible for this alteration were investigated.

CHAPTER 2

METHODOLOGY

2.1 The WBMsed model

The WBMsed framework is used in this study to develop the global-scale bedload model. It is an extension of the global-scale WBMplus hydrology model (Wisser et al., 2010). WBMsed features a spatially and temporally explicit (pixel-scale and daily) suspended sediment module based on the BQART river-mouth sediment load equation (Syvitski and Milliman, 2007), as part of the FrAMES biogeochemical modeling framework (Wollheim et al., 2008). WBMsed has been chosen here as a modeling framework considering its previous applicability for global-scale modeling.

Cohen et al. (2013) successfully estimated long-term average and inter-annual suspended sediment flux trend globally using WBMed. Results of the two validation procedures at 95 river mouths and using 11 years of daily sediment flux observations of 11 USGS stations lead us to conclude that WBMsed can successfully predict multi-yearly average sediment flux over diverse geographical settings. Moderate correlation between WBMsed and the observational dataset (R^2=.66) has been found for predicting long-term suspended sediment. This shows that the spatially and temporally explicit WBMsed is robust enough to be applied to predict long-term sediment trends. The results show that the model overestimates daily sediment flux by an order of magnitude during high discharge periods and that the mispredictions of the sediments are directly linked to the mispredictions of discharge. Later, this issue was addressed by Cohen et al. (2014), who introduced a floodplain component in the model to store overbank flow and get

more realistic riverine flood predictions, even during high and low flows. For this purpose, Cohen et al (2014) simulated sediment and discharge for the period of 1960-2010 to capture yearly trends (normalized departure from mean) at both pixel scale and continental scale. Syvitski et al. (2014) also used WBMsed to examine the role of climate in tropical discharge and sediment load and concluded that the WBMsed model can be used to demonstrate how tropical rivers behave under pristine conditions.

2.*2 Bedload Flux Module*

Here, the modified Bagnold (1966) equation (Syvitski and Saito, 2007) was used as a governing equation for the new bedload flux module, developed within the WBMsed framework. The main limitation of simulating any bedload formulae within WBMsed frameworks relates to the coarse resolution of WBMsed, which hinders explicit calculation of some of the equation's variables (e.g., sediment particle size, critical velocity). These variables were approximated based on parameters already available within the WBMsed framework, and coefficient values from previous studies (e.g., Begnold, 1966; Kettner and Syvitski, 2008). The modified version of the Bagnold equation has been extended by Kettner and Syvitski (2008) within the HydroTrend v.3.0 model to simulate daily bedload flux as a function of delta plain slope and the daily mean water discharge in river outlets, and is proposed here to use as the governing equation for the simulation:

$$\mathbf{Q_{b[i]}} = \left(\frac{\rho_s}{\rho_s - \rho}\right)\frac{\rho g Q^{\beta}[i] S e_b}{\mathbf{g}\tan\lambda} \textbf{ when } u \geq u_{cr} \qquad \textbf{(1)}$$

where, $Q_{b[i]}$ is bedload flux (kg/s), ρ_s is sediment density (here, sand density = 2670 (kg/m3)), ρ is fluid density (kg/m3 = 1000 kg/m3), g is acceleration due to gravity (m/s2 = 9.81), β is

bedload rating term (dimensionless = 1), e_b is bedload efficiency, defined as the ratio of the flow's capacity to do work to the amount of work done to move sediment and depends on the fluid (air or water) medium in which transport occurs (value can vary from 0.1 to 0.2, 0.1 is used here), *S* is gradient, (a new spatially explicit river slope (m/m) layer is used here), λ is dynamic coefficient of friction, calculated from limiting angle of repose of sediment grains lying on the river bed (Bagnold, 1966; Syvitski and Alcott, 1995) (for most sands it is approximately 33 degrees, for which λ=0.6 is used in this study; Bagnold, 1966), *u* is stream velocity (m/s), and ucr is critical velocity needed to initiate bedload transport (m/s). Following Syvitski and Saito (2007) and Kettner and Syvitski (2008), the use of the above-detailed constant values for most of the Eq. 1 variables, the modified Bagnold (1966) equation is simplified into having only two variables: Q and S. Here Q is simulated by the WBMsed model and S is based on a new input dataset (described below).

2.3 Simulation Input Datasets

The modeled river network used in this simulation was derived from the high-resolution gridded network HydroSHEDS using the SRTM elevation dataset. The input datasets include air temperature, precipitation, flow network, water discharge, bankfull discharge, soil parameters, growing season start, irrigation area fraction, irrigation intensity and efficiency, cloud cover, wind speed, reservoir capacity, small reservoir storage fraction, crop fraction, ice cover, population, maximum relief, and lithology factor. The precipitation dataset is obtained from the Global Precipitation Climate Center (GPCC), Germany (gpcc.dwd.de), using their "Full" product, which combines long-term precipitation climatology. The GPCC "Full" product is available at monthly time steps at a 30 arc-minute spatial resolution. Daily partitioning of the monthly precipitation totals was established by computing the daily fraction of the monthly

precipitation from the NCEP reanalysis product (Cohen et al., 2013 and 14). Air temperature data is collected from National Centers for Environmental Predictions (NCEP) (nco.ncep.noaa.gov) at daily time steps for the time period of 1948–2009, and it is available at 11-km spatial resolution (Cohen et al., 2013 and 14). One of the changing prominent parameters used in the Bagnold equation (1966) to predict bedload transport is discharge. WBMsed uses the WBMplus daily discharge (Q) predictions, which include the water balance/transport model first introduced by Vörösmarty et al. (1989), and was subsequently modified by Wisser et al. (2010). This discharge prediction has been found to perform quite well (R2=.66), considering the large spatial and temporal dynamics. A new dataset of Global River Slope (GloRS; Cohen et al., under review) is used for the slope parameter, S, in Eq. 1. GloRS is the first global-scale river slope layer (Figure 1). It is based on a calculation of elevation change along river reaches at a known (at a user-defined maximum) length (Figure 1). Cohen et al. (under review) found it to have a good correspondence to observed river slope using the observational dataset compiled as part of this study. More details about the source dataset, available spatial resolution, and data-available time periods for each specific input parameters are described by Cohen et al. (2013).

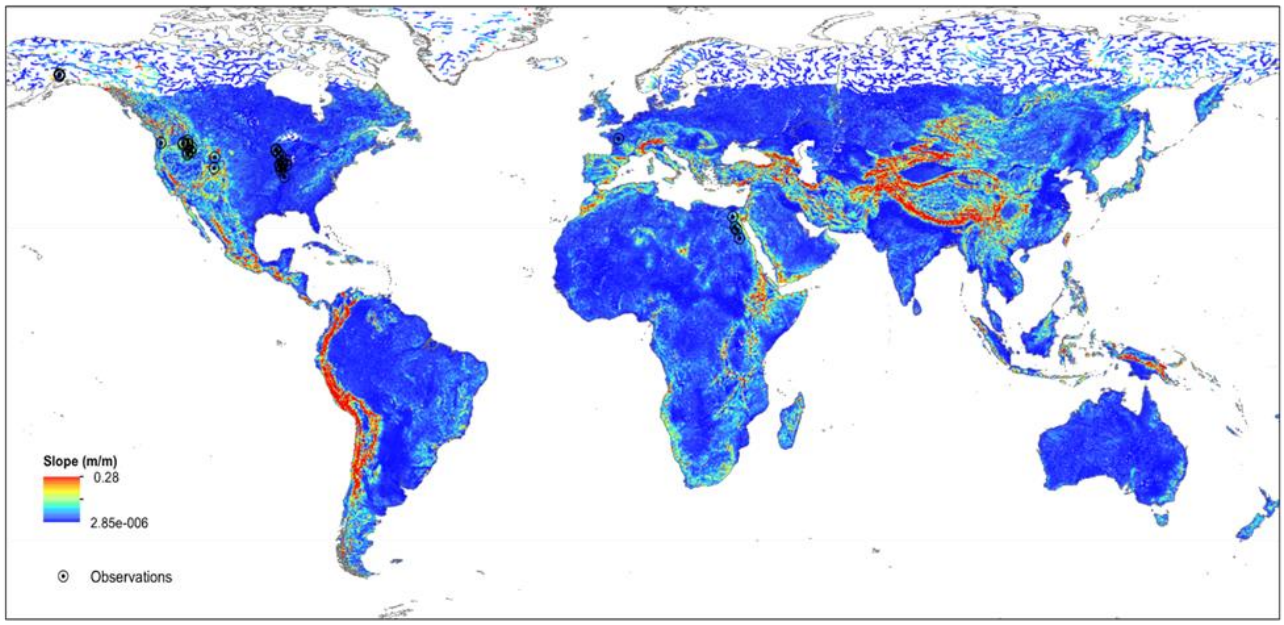

Figure 1: The Global River Slope Layer (GloRs) (Source: Cohen et al., under review) and location of observation sites for slope validation

2.4 Simulation Settings

The simulations conducted in this study are daily at 6 arc-min (~11 km at the equator) spatial resolution. Yearly and monthly averaged bedload flux and discharge output files were generated for a 41-year (1970–2010) simulated span to correspond to the observational database. The WBMsed framework has so-called 'pristine' simulation mode in which no anthropogenic parameters (e.g., irrigation, dams, land use) are included. The simulations conducted for this study were in 'pristine' mode as the WBMsed bedload module does not yet include anthropogenic parameters (primarily trapping behind dams). The results of the simulated hydrological parameters also represent 'pristine' conditions.

2.5 Model Validation

Even though WBMsed simulates daily bedload fluxes (given the framework-inherent time steps), in this study only long-term average results are analyzed. This is because the bedload module used cannot realistically robustly estimate complex temporal bedload dynamics at this scale. The validation analysis is therefore also based on the time-averaged comparison between observed and model-predicted bedload at 59 locations (Figure 2). The observational database was compiled from different organizations (e.g., U.S. Geological Survey, U.S. Army Corps of Engineers, U.S. Forest Service) and individual researchers. Two major sources used to compile the database are Williams and Rosgen (1989), the first comprehensive datasets for total sediment loads (suspended loads plus bedloads) for 93 streams across the United States; and Hinton et al. (2012), reportedly the most comprehensive database for bedload transport to this date that contains 15,018 observations from 484 datasets worldwide, but the number of big rivers and variations covered in this research makes it the most comprehensive dataset to this day. USGS reports were also found to be a rich source of such data, but most of the datasets mainly include observations from small rivers, streams, and creeks. Due to the coarse spatial resolution (6 arc-min) of the model, only data from basins with area more than 1,000 km^2 has been considered for the validation purpose. From an initial database of 111 sites, only 59 were used here. Observations from small rivers (< 1000 km^2) and those along the same river reach (often same model grid-cell) were removed to reduce spatial autocorrelation. The resulting observational database is dominated by sites in the U.S (57 out of 59; Table 1) due to reported data availability in this country. In addition to bedload flux, the database includes drainage area, discharge,

coordinates, and, for some sites (24), river slope. These secondary variables were used for analyzing the sources of bias in the model predictions.

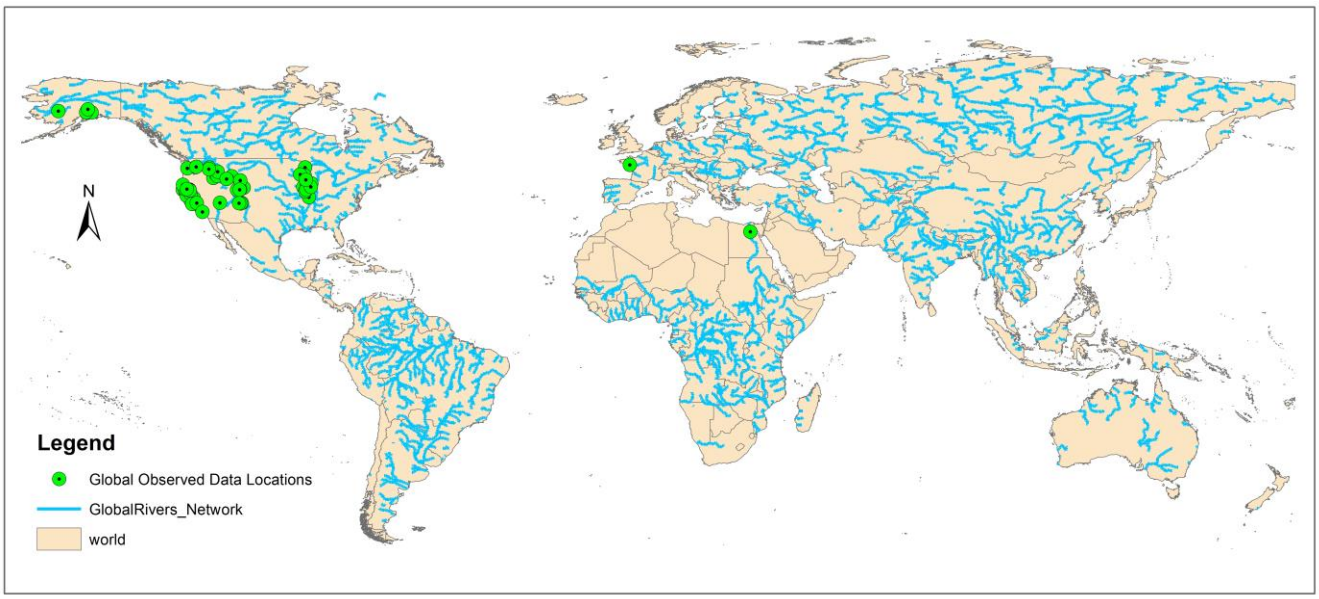

Figure 2: Observed Bedload Data Locations Maps used for Validation

Table 1: Observational Database

Data Set Name	State or Country	Latitude	Longitude	Basin Area (km^2)	Observed Discharge (m^3/s)	Observed Bedload (kg/s)
Knik River	AK	61.51	-149.03	3056.19	522.00	60.68
Kuskokwim River	AK	61.87	-158.11	80500.00	2701.25	37.24
Susitna River at Sunshine	AK	62.18	-150.17	28700.00	1579.33	37.23
Susitna River at Susitna Station	AK	61.54	-150.51	50200.00	2500.44	73.50
Talkeetna River	AK	62.35	-150.02	5205.88	273.60	12.00
Virgin River	AZ	36.89	-113.92	13182.59	40.78	3.01
Mad River	CA	40.85	-123.98	1256.14	109.32	17.71
Stony Creek	CA	39.74	-122.37	1613.56	8.45	0.44
Cow Creek	CA	40.51	-122.23	1100.74	53.35	0.91
Alameda Creek	CA	37.59	-121.96	1639.46	22.64	1.91
Cache Creek	CA	38.75	-122.07	2696.18	140.50	3.50
Cottonwood Creek	CA	40.39	-122.24	2400.92	57.93	2.56
Eel River	CA	40.49	-124.10	8062.67	424.83	34.67
Middle Fork Eel River	CA	39.71	-123.32	1367.51	56.49	8.50
Mokelumne River	CA	38.24	-121.08	1711.98	0.85	0.01
Russian River Cloverdale	CA	38.88	-123.05	1302.76	136.83	18.17
Sacramento River Butte City	CA	39.46	-121.99	31274.25	297.60	0.72
Sacramento River Near Red Bluff	CA	40.29	-122.19	23050.89	272.32	2.08
Salinas River	CA	36.55	-121.55	10468.73	309.00	20.90
San Joaquin Below Chowchilla	CA	36.83	-120.26	4718.96	23.15	7.08

Santa Clara River	CA	34.42	-118.72	1618.74	1.75	0.79
South Fork Trinity River	CA	40.65	-123.49	1978.75	69.50	13.56
Smith River	CA	41.79	-124.08	1590.25	107.35	0.45
Trinity River	CA	40.65	-122.96	2411.28	155.08	1.90
Green River Lodore	CO	41.04	-107.87	8243.93	160.97	9.61
Little Snake Lily	CO	40.55	-108.42	10448.01	16.98	4.48
Yampa River	CO	40.45	-108.52	20541.20	196.00	13.46
Bani-Swef, Nile River	Egypt	29.06	31.10	3049558.00	1040.00	3.92
Loire River	France	47.27	-1.90	117000.00	950.11	28.51
Iowa River	IA	41.18	-91.18	32374.85	405.50	15.06
Boise River	ID	43.67	-115.73	2154.87	106.48	2.03
Clearwater River	ID	46.45	-116.83	24042.86	1234.66	2.59
Middle Fork Salmon River	ID	44.73	-115.02	2693.33	282.81	6.97
Salmon Below Yankee Fork	ID	44.24	-114.67	2100.54	78.25	0.29
Salmon River Near Shoup	ID	45.35	-114.55	16151.40	434.08	8.97
Snake River near Shelley	ID	43.41	-112.14	25355.98	157.78	0.00
Green River Geneseo	IL	41.49	-90.16	2597.76	140.90	1.13
Henderson Creek	IL	41.00	-90.85	1118.87	67.87	2.38
Kaskaskia River	IL	38.45	-89.63	11377.82	23.84	0.03
Kishwaukee River	IL	42.21	-88.99	2846.40	88.35	1.69
La Moine River	IL	40.02	-90.63	3348.85	137.62	1.59
Rock River	IL	41.56	-90.19	24731.80	23.32	5.74
Spoon River at Seville	IL	40.49	-90.34	4237.22	245.79	5.22
Vermilion River	IL	41.24	-89.05	3240.08	10.26	0.24

Animas River	NM	36.86	-107.96	3522.38	6.10	0.01
San Juan at Farmington	NM	36.72	-108.23	18751.51	21.75	0.34
San Juan at Shiprock	NM	36.78	-108.68	33410.85	21.00	0.12
Green River Jensen	UT	40.41	-109.23	76819.05	242.20	6.31
Naches River	WA	46.63	-120.51	2864.53	244.00	12.29
Snake River near Anatone	WA	46.10	-116.98	240765.29	2282.18	11.35
Toutle River	WA	46.34	-122.84	1284.63	113.04	61.46
Yakima River	WA	46.72	-120.45	5537.40	179.67	1.10
Bad River	WI	46.53	-90.64	1546.22	137.00	0.16
Black River	WI	44.35	-90.75	5387.18	57.63	1.76
Chippewa River	WI	44.63	-91.97	23335.79	290.88	8.55
Wisconsin River	WI	43.20	-90.44	26935.87	303.30	10.25
Snake river	WY	44.10	-110.67	1258.73	77.88	1.15
Little Snake Dixon	WY	41.04	-107.45	2558.91	75.29	1.00
Wind River	WY	43.01	-108.38	5980.31	113.82	2.58

2.6 Evaluating Bedload Sensitivity to Key Parameters

Bedload flux depends on various parameters such as velocity, depth, and sediment particle size (especially the median grain size). Most of the bedload flux equations are one-dimensional and nonlinear and involve local hydraulic parameters. Also, most bedload formulas were almost exclusively developed based on lab experiments and on field observations in small rivers and streams, in which hydraulic characteristics were controlled or could have been well-approximated. The modified Bagnold (1966) equation, used in this study, simplifies these fine-

scale parameters by using discharge and slope as a proxy for these fine-scale parameters. The feasibility of this approach for the spatial and temporal resolutions used in global-scale modeling is a major focus of this study. Besides, the influence of several hydraulic and geologic parameters (lithology, trapping efficiency, water temperature, suspended sediment, basin area, stream length, stream order, and topographic slope) on bedload flux was tested using bi-variate and multi-variate regression analysis. This is similar to Syvitski and Milliman's (2007) development of the semi-empirical BQART suspended sediment equation.

The observational dataset was used to extract point values from eight global layers. The topographic slope was extracted from a global-scale basin slope layer, which was calculated based on a high-resolution DEM (Digital Elevation Model), upscaled to 6 arc-min resolution, and was used to calculate the upstream average basin slope for each grid-cell. The WBMsed lithology erosivity layer (Cohen et al., 2013) was used. Stream length represents the flow distance of each grid-cell from its most upstream cell. Stream order has been used to find whether confluences have any impact on bedload transport. The observed basin area is used to find the general trend of sediment transport as the area increases, and is collected for all the sites from secondary sources (e.g., reports). Water temperature (Cohen et al., 2013) is used as bedload transport is expected to increase with increasing temperature. Also, a trapping efficiency layer for each pixel was considered to find the relative importance for influencing bedload transport. Lastly, the average suspended sediment (Qs) is used to find the correlation with bedload flux, run in the WBMsed framework by Cohen et al. (2014), as generally rivers with high sediment tend to have high bedload transport due to increasing discharge rate. Lastly, the discharge, the main driver for bedload flux, was considered with other parameters to find any combination of these parameters that can improve the predictability of bedload flux.

2.7 Analysis of the Suspended and Bedload Flux Dynamics along the Main Stem of Large Rivers

Conceptually, the percent of sediment transported in suspension increases downstream, with bedload dominating steep headwater streams, and suspended flux dominating (~90%) coastal rivers. However, few studies have focused on this difference (Sadeghi and Kheifam, 2015), primarily due to data limitations. Focusing on large rivers (>1,000 km^2), it is hypothesized for this study that suspended to bedload percentage will show quantifiable and universal trends, and their ratio is dominated by basin characteristics (e.g., stream length, slope) (Turowsky et al., 2010). To elucidate this spatial dynamic between suspended and bedload fluxes and the influence of basin characteristics, the amount of suspended and bedload flux is calculated for each grid cell, after completing the validation process of the global bedload flux model. Then the percentage of bedload flux in total sediment flux is shown in a normalized scale of stream length against bedload percentage for four large rivers (Mississippi, Ob, Yangtze, and Ganges). A quantitative analysis of spatial dynamics of these sediments and the driving factors for the spatial dynamics is also discussed.

CHAPTER 3

RESULTS AND DISCUSSION

3.1 Global Daily Long-Term Bedload Flux Trend

The global bedload flux (6 arc-minute) output for large rivers (basin area > 20,000 km^2, and discharge > 30 m^3/s) is shown in Figure 4. This subset of large rivers was done considering that the main focus of this research is determining bedload flux for large rivers. Moreover, to get full comprehension of all the rivers with high variability in the same platform is difficult and sometimes confusing. Each streamline in the map represents daily long-term (1970-2010) mean bedload flux predictions for each specific river.

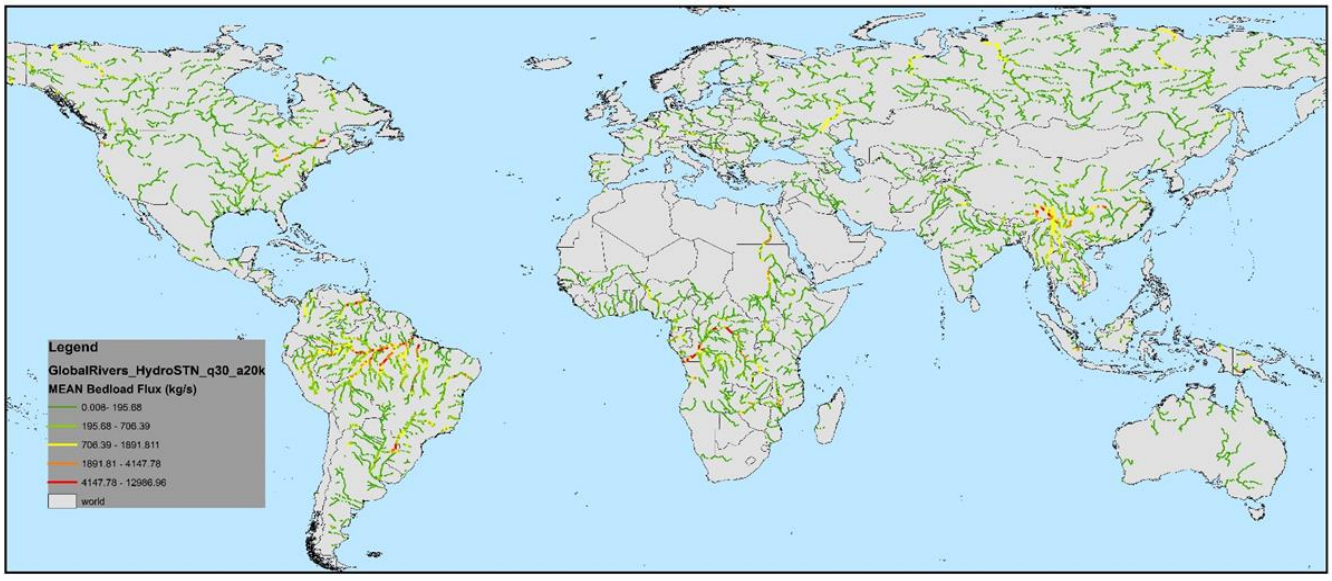

Figure 3: Long-term daily average bedload flux map for large rivers

The mean value of bedload flux is 254.9 (kg/s), with a standard deviation of 3452.3 (kg/s). The high standard deviation is expected because a few large rivers (e.g., Amazon) with high bedload transport rate influence the deviation from the mean. The median bedload flux value is only 8.87 (kg/s), which means that half of the rivers have bedload flux lower than this transport rate.

Rivers in tropical areas, including South American, African, and Asian rivers, show high bedload transport, mostly due to high water discharge (Syvitski et al., 2014) as a result of high rainfall, especially during summer. Rivers of South America, including the Orinoco, Amazon, and Parana **(Figure 4),** show high bedload flux mostly because these streams are located in tropical areas, which are subject to humid temperature with high rainfall intensities, and the bedrock of rivers in these areas are susceptible to erosion, resulting in high bedload flux, as mentioned by Syvitski et al. (2014). As South American rivers are most affected by tropical climates, high bedload flux with a mean of 1448.84 (kg/s) and median value of 101.4 (kg/s) is observed for this continent.

In Africa, the Congo and Nile rivers show high bedload flux, as these rivers flow through high topographic land and have higher slopes, which influence bedload transport. In Asia, the Yangtze River shows high bedload flux because its stream path runs through a deep valley, and in addition, it gets high precipitation during summer as and high velocity in high topographic areas.

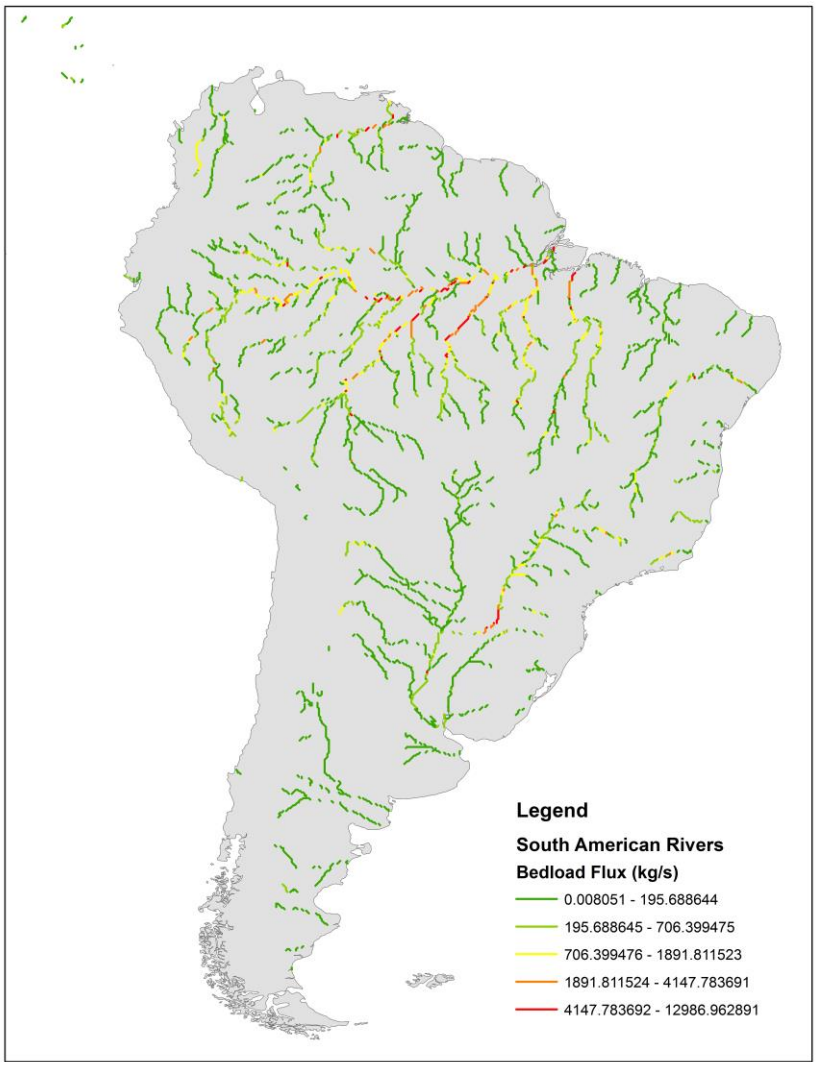

Figure 4: South American Rivers showing Bedload Transport

Figure 5, shows bedload yield (kg/sec/km^2) calculated by dividing the bedload output (kg/s) with corresponding drainage area (km^2). High bedload transport rate in tropical regions, along with high topographic areas are visible due to the high slope, and strong rainfall in these areas.

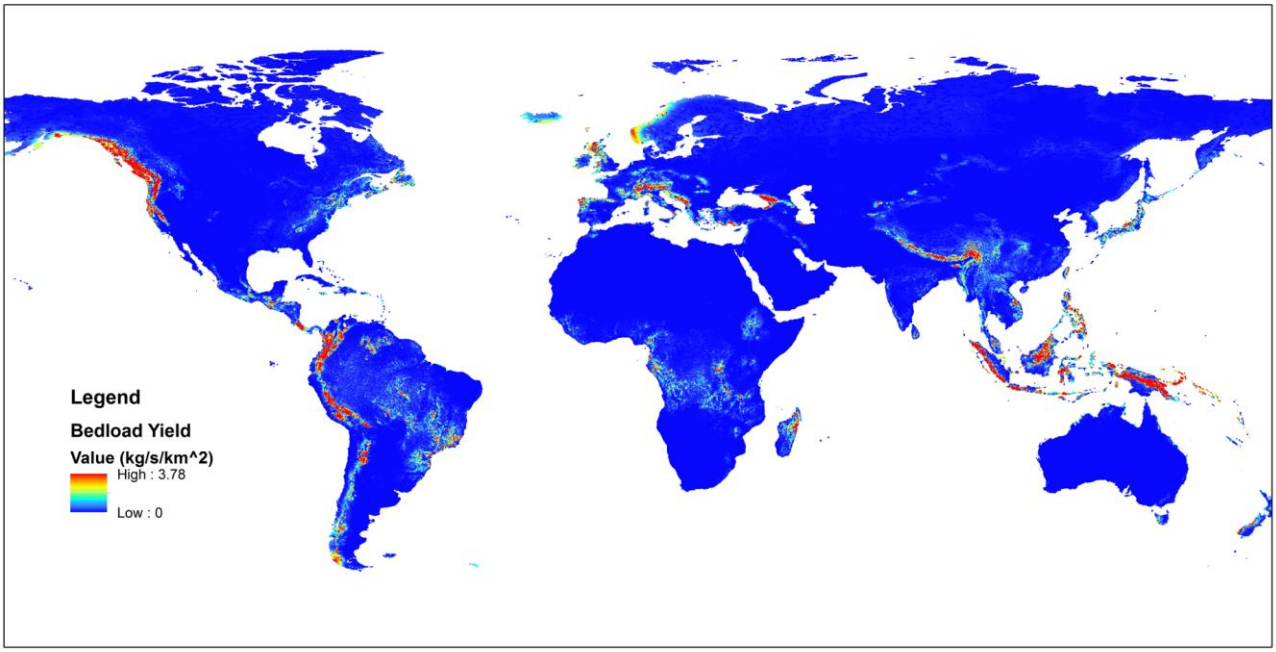

Figure 5: Bedload Yield Map

3.2 Model Validation:

In the validation procedure, I tested how the spatially explicit calculation of bedload flux by WBMsed performed compared to observed bedload flux. The observational database was subset based on the following criteria: basin area larger than 1,000 km^2, rivers that have a discrepancy of less than 10% between actual river basin area and WBMsed calculated drainage area, and avoided data representing the same stream network to minimize intercorrelation within the data themselves. The observational data for each location represents the average of all the daily bedload flux values reported for each site. This was done by extracting daily WBMsed values corresponding to the daily observational values for each site. These values were then averaged, yielding one modeled and one observed value per observational site. The amount of observed daily data varies in each location. Correlation analysis (log-log) between these daily averages was used for quantifying the model accuracy. A log-log analysis is used given the ~5 order of magnitude range of the data.

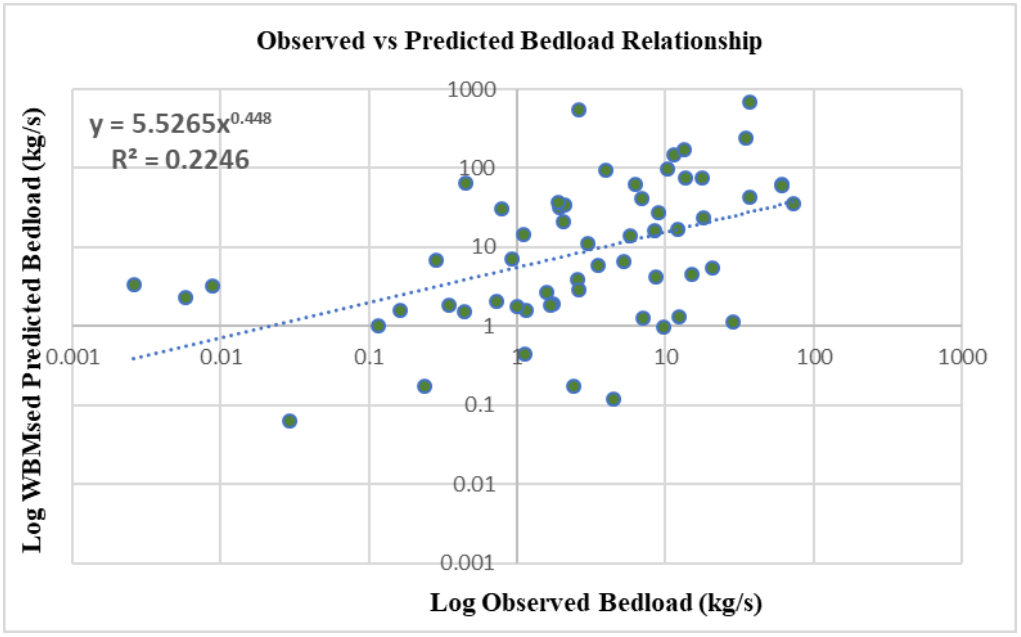

Figure 6: WBMsed Model bedload flux relationship with Observed Bedload

Overall WBMsed predictions correspond moderately to observed bedload flux data with R^2=0.22 **(Figure 6).** WBMsed overpredicted bedload transport for most of the locations, due to the limitation of reservoir trapping capabilities within the modeling framework. The model is not capable yet to consider the anthropogenic impact on bedload, so considering this limitation the results seem reasonable. Also, observational data includes bedload of five orders of magnitude. To get high correlation and accurate prediction within this type of high-variability observations, data needs to be considered in different categories (e.g., large, medium, and small rivers). But here, this method is not followed, considering limited observational data for large rivers (>20,000 km^2) which is the main focus of this research.

From the bias in bedload flux and observed bedload relationship graph **(Figure 7),** high bias in the prediction (three orders of magnitude) is found. This high bias is due to higher variability in observed bedload data (five orders of magnitude), as has already been mentioned. Most of the observed bedload flux values greater than 10 kg/s, show relatively low bias (two orders) compared with the overall bias result. So, this high bias can be reduced if the model considers rivers of different orders of magnitude based on their relative basin area, discharge, and observed bedload flux.

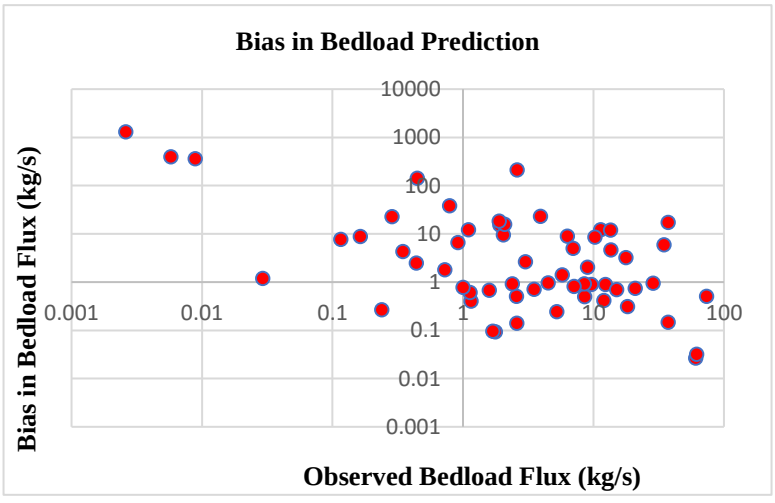

Figure 7: Bias vs Observed Bedload Flux

3.3 Investigation of Bias Cause in Bedload Prediction

At its current formulation, only two dynamic variables (discharge and slope) control the spatial and temporal variability in the model's bedload calculations, along with several constant parameters. The correlation between observed bedload and these two variables can therefore be useful for evaluating their overall influence. Observed bedload shows moderate correlation (R^2=0.38; **Figure 8**) with observed discharge. This means that discharge explains about 38% of the variability in bedload transport, which is quite high.

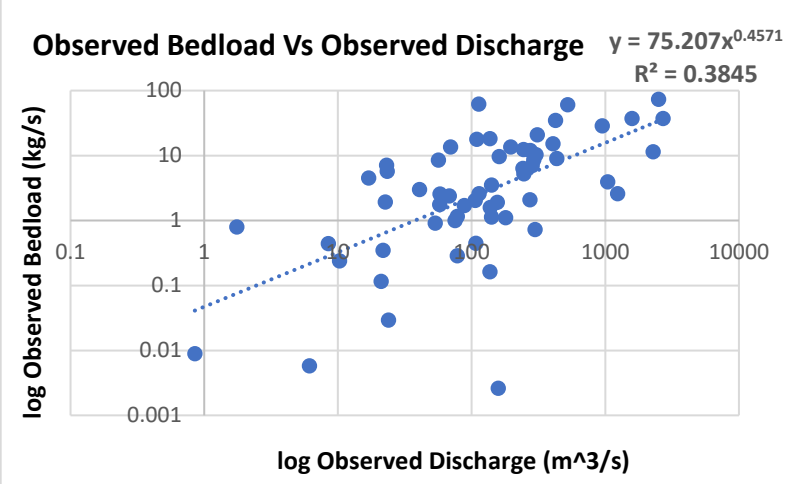

Figure 8: Observed bedload vs Discharge Relationship

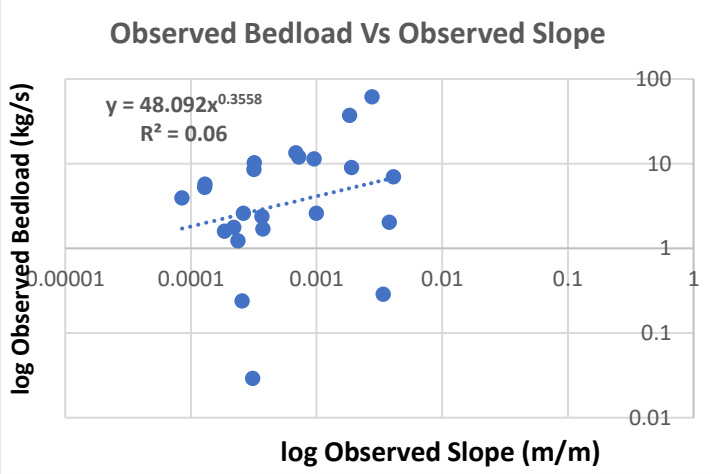

Figure 9. Observed Bedload vs Slope relationship

To find the correlation between observed bedload and observed slope, a subset of the observed data (24 out of 59) was considered, because observed river slope (bed or water) is only available for these locations. The correlation between observed bedload and slope is very low (R2=0.06; **Figure 9**). This is surprising because slope could be considered as a proxy for the potential transport energy of the river flow. That is why, for example, mountainous rivers have

greater bedload yield **(Figure 5)**. This result suggests that river slope is not contributing as expected for bedload prediction, so further clarification is needed.

Comparisons between model-predicted and observed discharge show a moderate correlation (R^2=0.45; **Figure 10**). Previous evaluation of WBMsed showed that its predictive skills are much higher for discharge (~R^2=0.75; Cohen et al., 2013). The lower skills, in this case, are likely because these results are based on 'pristine' simulations, which do not take into account anthropogenic drivers. A slightly higher correlation was found for slope (R^2=0.50; **Figure 11**). This is also lower than the comparison conducted by Cohen at al. (2017) for the GloRS dataset which was used as input to the model. This may be explained by the fact that the validation dataset used in the Cohen et al. (2017) study was slightly different. These moderate predictions of the two main parameters of the model's governing bedload equation explain a large proportion of the bias in the bedload predictive skills. Based on this understanding, we can assume that improving both the river slope input and improving the model discharge predictions have the potential for considerably improving WBMsed bedload predictions.

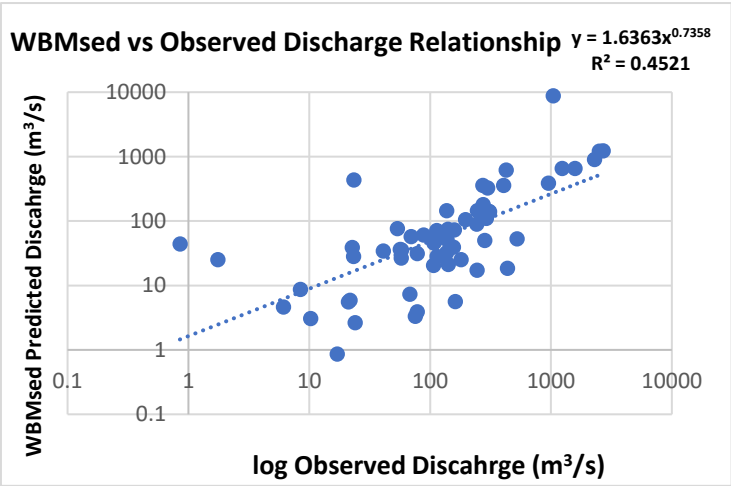

Figure 10: WBMsed Vs Observed Discharge

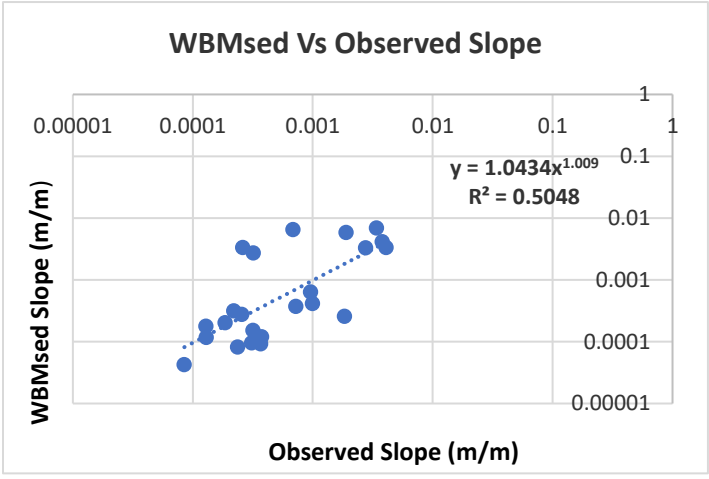

Figure 11: WBMsed Vs Observed Slope

To further investigate the slope influence on bedload flux, different constant slope values (ranging from 0.000001 to 0.1) were used to manually calculate the model's governing bedload equation (modified Bagnold, 1966) using observed discharge. The correlation between the manually calculated equation with constant slopes and observed bedload yielded a moderate correlation (R^2=0.39; **Figure 12**). Different constant slope values affected overall correspondence values, first with increasing slope value from 0.000001 started to increase the 1:1 relationship. The best 1:1 relationship was found for slope value of 0.0001. After this value, the 1:1 relationship started to decrease. Within this high range of slope values applied here, the overall correlation remains the same (R^2=.39). Considering the low influence of these different slope values on bedload prediction, it can be concluded that constant slope has a very low impact on bedload, and it cannot improve bedload flux prediction significantly.

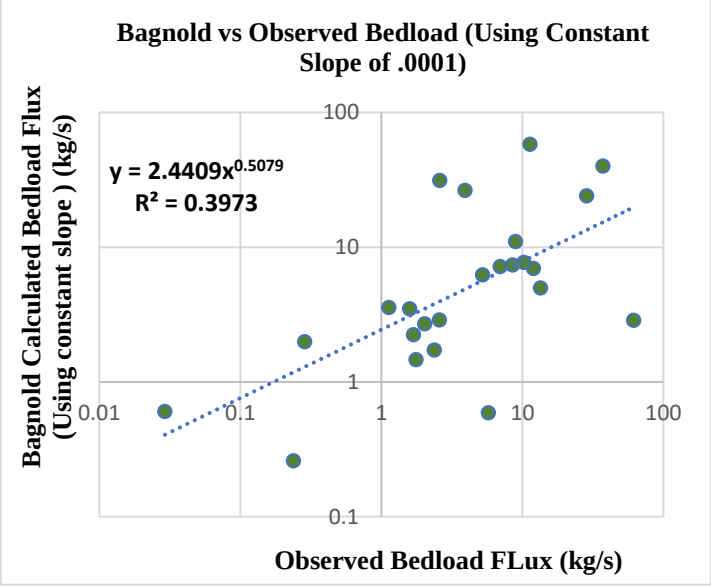

Figure 12: Bagnold vs Observed Bedload (using constant slope)

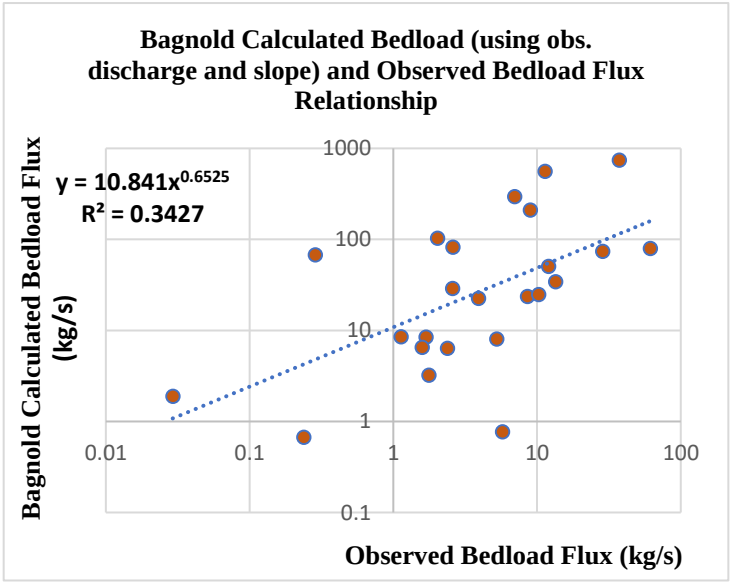

Figure 13: Bagnold vs Observed Bedload (using observed discharge and slope)

Manually calculating the equation with both observed discharge and slope, a moderate correlation of R^2=0.34 has been found (Figure 14). This confirms that the spatially distributed slope does not improve bedload prediction significantly. This may because, due to the low resolution of the model input, slope is not contributing significantly at this resolution. So, an alternative and better variable to represent explicit stream power at this resolution of the model may be necessary.

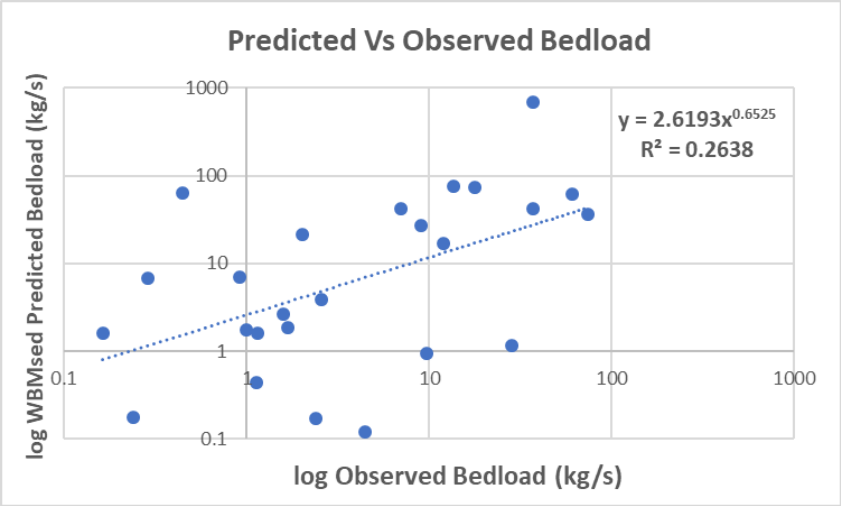

Figure 14: WBMsed Vs Observed Bedload for Locations with Zero Trapping Efficiency

Lastly, the relationship of WBMsed Vs Observed Bedload with zero trapping efficiency location has been investigated. The R^2 value improve a little bit (from .22 to .26), but as the number of observations has been reduced considerably (from 59 to 25) this increase cannot be accepted with high confidence.

3.4 Determining the Influence of different Variables on Bedload

Bedload transport may be influenced by other variables, not included in the current WBMsed equation, such as lithology, topography, shear stress, particle size, water temperature, etc. Here, in addition to the previous two variables (discharge and river slope), several new variables (lithology, trapping efficiency, water temperature, topographic slope, suspended sediment, drainage area, stream length, and stream order) were explored to find the relationship of these variables with observed bedload flux. All these variables have been collected from previous studies and available datasets within the WBMsed framework.

3.4.1 Lithology: Sediment travels within watersheds from headwaters to downstream, evolves within the stream channel, and is eventually deposited into oceans. During this travel, the abrasion characteristics of different rock types within the stream network can influence sediment dynamics, especially downstream (Pizzuto, 1995; Attal and Lavé, 2006; Sklar et al., 2006; Chatanantavet et al., 2010; O'Connor et al., 2014; Cox and Nibourel, 2015; Menting et al., 2015). To determine the influence of lithology on bedload, upstream-averaged lithology erosivity factor was extracted from WBMsed. The WBMsed suspended sediment lithology parameter has range from 0.3 to 3, where 0.3 represents hard rock, and 3 represents softer lithology (Cohen et al., 2013). A very weak relationship was identified between bedload flux and lithology **(Figure 15).**

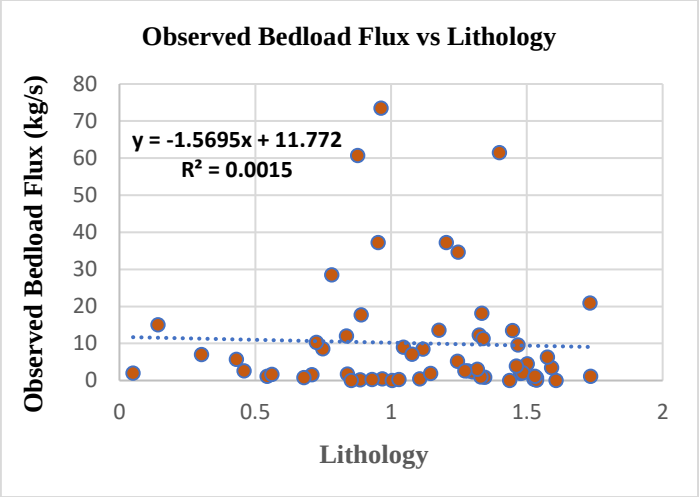

Figure 15: Relationship of Lithology with Bedload

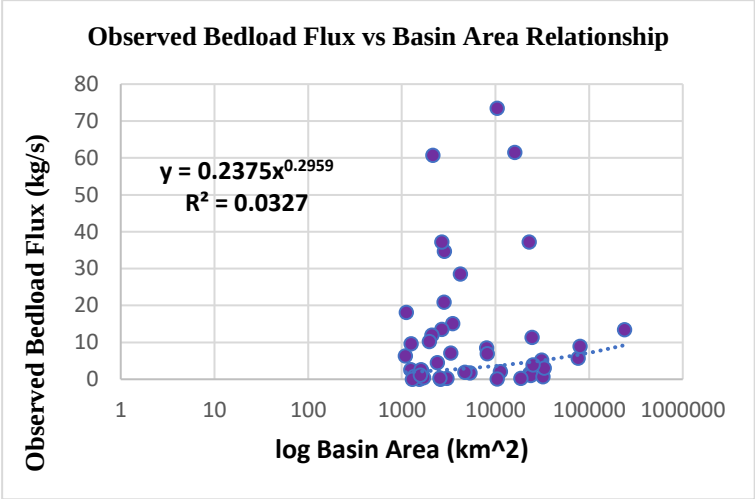

Figure 16: Relationship of Basin Area with Bedload

3.4.2 Basin Area: Conventionally, sediment transport increases as basin area increases, as increased basin area generally leads to higher water discharge. This is more applicable for the rivers where the main source of sediment is basin erosion. From the above bedload flux and basin area relation **(figure 16),** a similar result has been found. Although very low correlation (R2=.03) was found, the positive trend shows that the sediment transport will increase downstream with the increased basin area.

3.4.3 Water Temperature: Effects of water temperature on bedload transport give very conflicting results (Akalin, 2006; Hong, 1984). Some researchers such as Ho (1939) concluded that bedload particle transport decreases at colder water temperatures, whereas Mostafa (1949) determined that the sediment transport increases with the increasing water temperature. To conclude this conflict, later studies were conducted and concluded that, if other variables are constant, then sediment transport will decrease with increasing temperature mainly due to the drop in fluid viscosity (vvihsd,2016). Moreover, the studies also found that the effects of

temperature can vary for bedload transport based on the sediment grain size. Here, a decreasing trend was found for temperature, but with very low correlation (R^2=0.06; **Figure 17**).

3.4.4 Stream Length: For suspended sediment, as the length of the stream increases from headwaters, the sediment transport increases, particularly for rivers dependent on basin erosion as a sediment source and with diverse land use. This is also true for bedload; most of the time bedload increases with increasing stream length. This happens as more water gets added to rivers from its tributaries. Here, a similar trend has been observed from the bedload flux and stream length relationship (**Figure 18**) with low R^2 of 0.03.

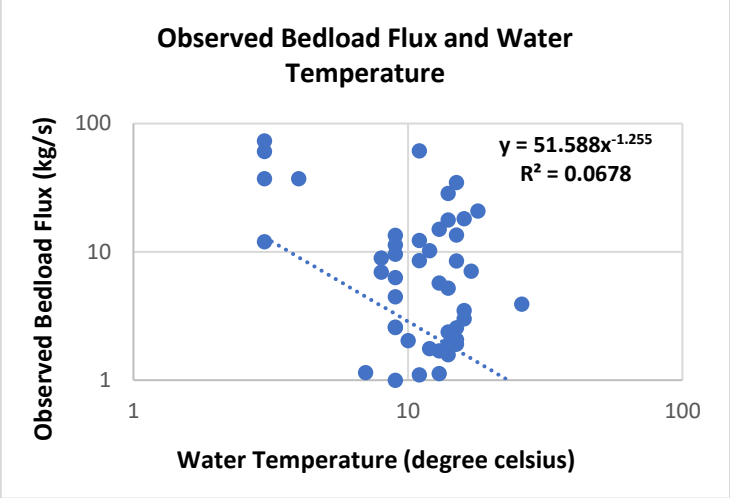

Figure 17: Relationship of Water Temperature with Bedload

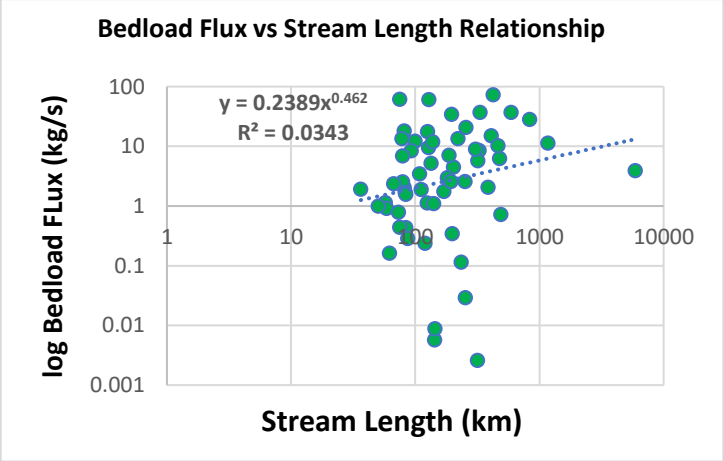

Figure 18: Relationship of Stream Length with Bedload

3.4.5 Stream Order: Rivers with higher stream order are expected to have higher bedload transport than those with lower order, as in higher stream orders more water and sediment get added from their lower-order tributaries. Here, a similar positive trend was found with a low R^2 of 0.04.

3.4.6 Topographic Slope: Topographic slope, generated from a DEM, represents the average upstream landscape slope instead of local river slope. No significant correlation between topographic slope and bedload was found (R^2=.0007).

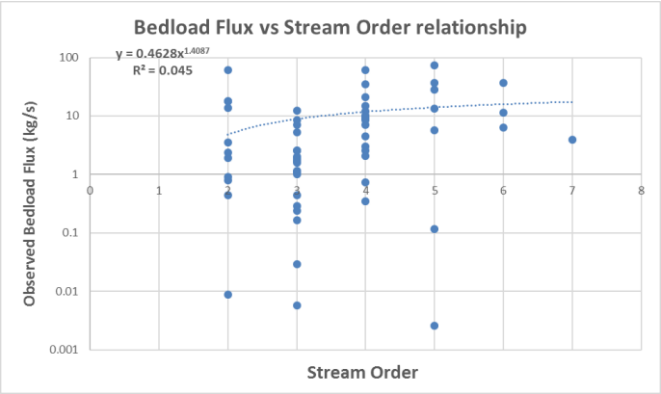

Figure 19: Relationship of Stream Order with Bedload

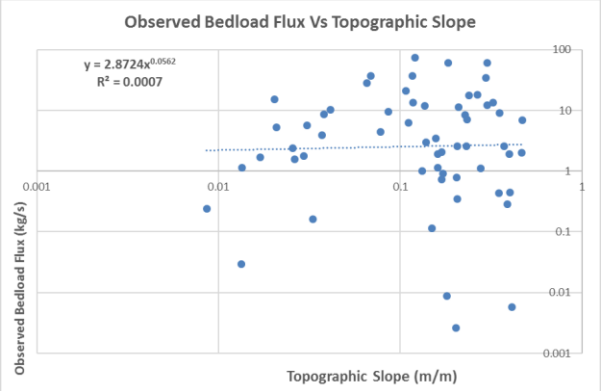

Figure 20: Relationship of Topographic Slope with Bedload

3.4.7 Trapping Efficiency: Dams and reservoirs can trap a significant portion of sediment, which otherwise would have been delivered to the oceans (Syvitski et al., 2005; Vorosmarty et al., 2003). The layer of trapping efficiency of the reservoirs, used here is calculated by Kettner and Syvitski (2008) based on the reservoir locations within the river network, and the volume of the reservoirs that determines the amount of time water remains within the reservoir. They used three different equations Brown (1943), Brune (1953), and Vorosmarty (1997) to calculate trapping efficiency based on the different volumes of the reservoir. The trapping efficiency value, used here for each large reservoir is the sum of trapping value of reservoirs located within the sub-basin. A decreasing trend wasfound (**Figure 21**) with an R^2 of 0.04, which shows that trapping efficiency reduces bedload transport.

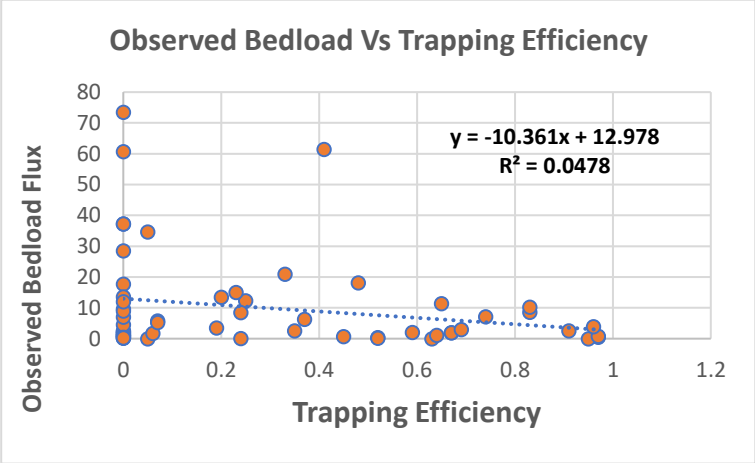

Figure 21: Relationship of Trapping Efficiency with Bedload Flux

A multi-regression analysis was conducted between bedload flux as the dependent variable (n=59) and lithology, basin area, water temperature, stream length, stream order, suspended sediment flux, and topographic slope as independent variables (Table 2). The main purpose of this analysis is to identify potential linkages between bedload flux and its controlling factors, which can lead to broader understanding of this complex phenomena. Log-converted values for both the dependent and independent variables were used. In the last step, a step-wise multiple-regression analysis was conducted that included all listed parameters. Not surprisingly (based on the results above), only discharge was identified as a significant controlling parameter with an R^2 of .38 which corresponds to previous findings of this study.

Table 2: Stepwise Multiple Regression Output

Excluded Variables[a]

Model		Beta In	t	Sig.	Partial Correlation	Collinearity Statistics		
						Tolerance	VIF	Minimum Tolerance
1	logWaterTemp	.001[b]	.005	.996	.001	.823	1.215	.823
	logSuspended	-.084[b]	-.707	.482	-.094	.779	1.284	.779
	logBasinArea	-.196[b]	-1.625	.110	-.212	.724	1.382	.724
	logStreamLen	-.168[b]	-1.412	.164	-.185	.748	1.336	.748
	logStreamOrder	-.169[b]	-1.386	.171	-.182	.712	1.404	.712
	logLithology	-.055[b]	-.529	.599	-.071	.996	1.004	.996
	LogTopographic slope	.040[b]	.385	.702	.051	1.000	1.000	1.000

a. Dependent Variable: logobsBedload

b. Predictors in the Model: (Constant), logobsDischarge

Model Summary

Model	R	R Square	Adjusted R Square	Std. Error of the Estimate	Durbin-Watson
1	.620[a]	.384	.374	.756	1.917

3.5 Sediment Flux Dynamics in the Main Stem of Selected Large Global Rivers

3.5.1 Mississippi River: The Mississippi, largest river basin in the United States, transport higher sediment than other rivers in North America (Meade et al., 1990). This river flows from northern Minnesota to Gulf of Mexico. **Figure 22(a) and (b)** shows the longitudinal profile of the Mississippi River, and the amount of sediment (both suspended and bedload) transported by the main stem is represented by different colors (dark blue represents low flux and dark red indicates high flux). The trends in stream length and sediment flux (both suspended and bedload) is shown in the **Figure 22 (e)**, where normalized stream length (0-1) is represented on the x-axis, suspended flux is represented on the y-axis, and bedload flux on the secondary y-axis. Lower values on the x-axis (starts from 0) indicate the upstream of the river, and the highest values (up

to 1) indicate the downstream of the river. On the secondary y-axis, bedload flux is represented in orange. Fluctuations in bedload flux values were smoothed to allow clearer comparison. For both suspended and bedload, the downstream Mississippi River shows high sediment flux, whereas upstream shows relatively low sediment flux. Especially for suspended sediment, a rapidly increasing pattern of suspended sediment is observed downstream because of the high influx of sediment from the Missouri River and Ohio River. Bedload flux also increases gradually, mainly due to the high-water flows resulting from the confluence of the river stem and its tributaries. Bedload flux near the outlet of the Mississippi decreases mostly due to decrease in slope.

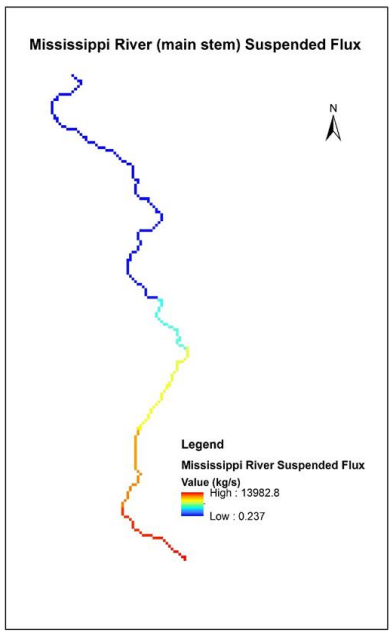

(a)

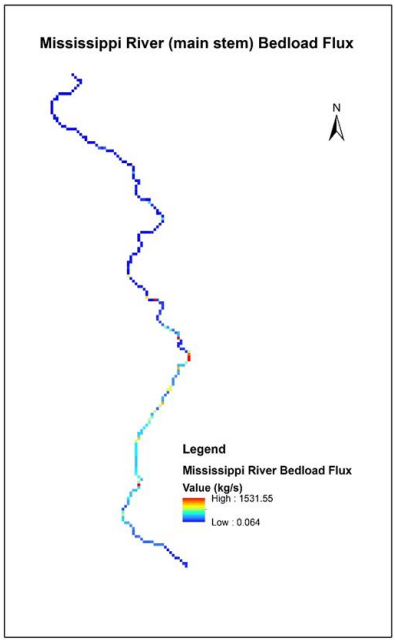

(b)

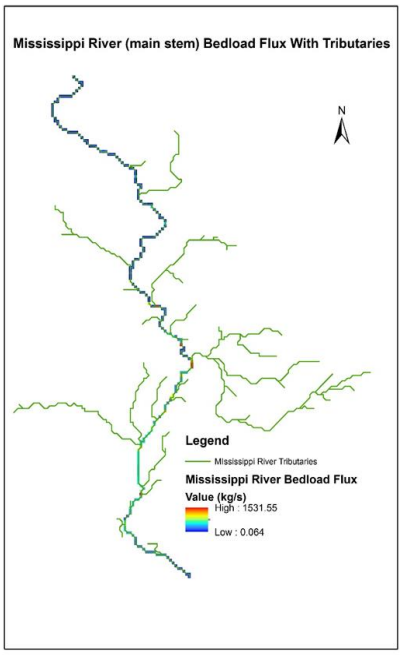

(c)

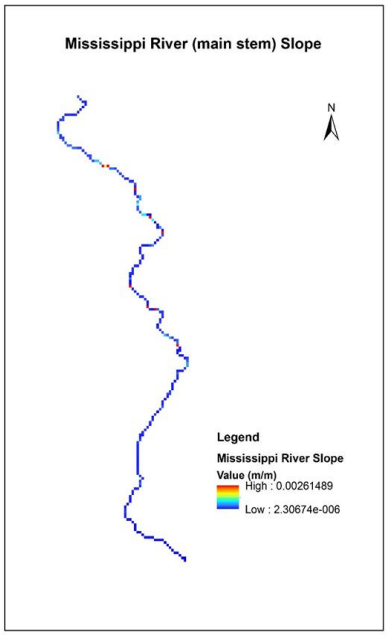

(d)

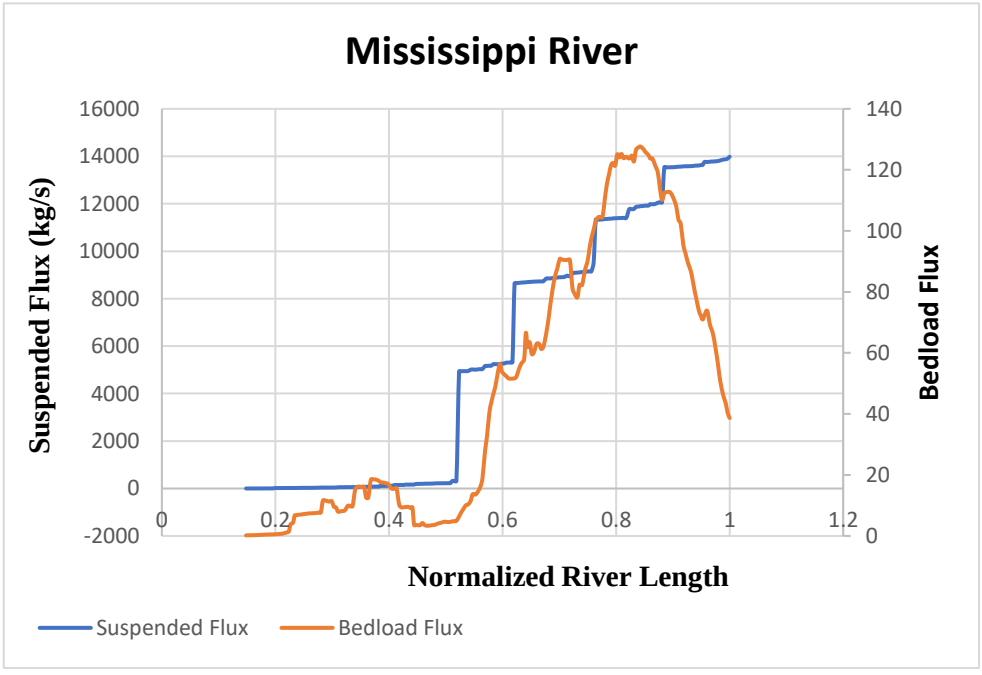

(e)

Figure 22: Longitudinal profile of Mississippi River (In upper row from left to right represents (a) suspended flux, (b) bedload flux, (c) Bedload flux with Tributaries, and in lower row from left to right (d) slope and (e) Relationship graph of bedload and suspended flux with normalized stream length

3.5.2 Yangtze River: The Yangtze, the longest river in Asia, ranks fourth in term of sediment flux in the world. It originates on the Tibetan Plateau and drains to the East China Sea. While flowing through deep valleys, the river makes some abrupt turns in the eastern part of the river. Due to this steep topography, and high precipitation in the eastern Tibetan Plateau, the eastern part of the Yangtze River shows high runoff as well as a high erosion rate. As a result of the high erosion rate, in the eastern part of the river, high sediment flux is observed. **Figure 23 (a), and (b)** shows the longitudinal profile of Yangtze River, and the amount of sediment (both suspended and bedload) transported by the main stem is represented by different colors (dark blue represents low flux and dark red indicates high flux). Also, the relationship of stream length and sediment flux (both suspended and bedload) is displayed in **Figure 23 (e)**, where normalized stream length (0-1) is represented on the x-axis, suspended flux is represented on the y-axis, and bedload on the secondary y-axis. Similarly, to the Mississippi River, here also lower values on the x-axis (starts from 0) indicate the upstream of the river, and highest values (up to 1) indicate the downstream of the river and will continue in a similar manner for the following rivers. On the secondary y-axis, bedload flux is represented in orange, and the highly fluctuating bedload flux has been smoothed to get a normal trend for better comprehension. From both longitudinal figures, as well as from the stream length and sediment flux (both suspended and bedload) relationship, suspended sediment shows a gradual increase downstream, shown in dark blue c in **Figure 23 (e)**. But bedload shows more flux in the middle part of the river due to an abrupt turn caused by deep valleys. As a result, high slopes in this area (**Figure 23 (d))** have more bedload flux, in addition to high discharge due to precipitation in this eastern part of the river and additional water flow added by tributaries (shown in **Figure 23 (c)**). Similar to bedload flux,

precipitation and higher topography in the eastern part of the river influence continuous increase of sediment flux in the eastern part of the river.

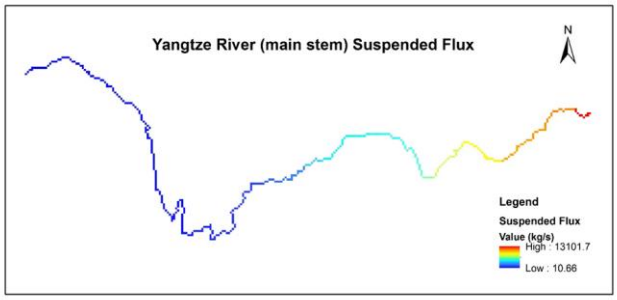

(a)

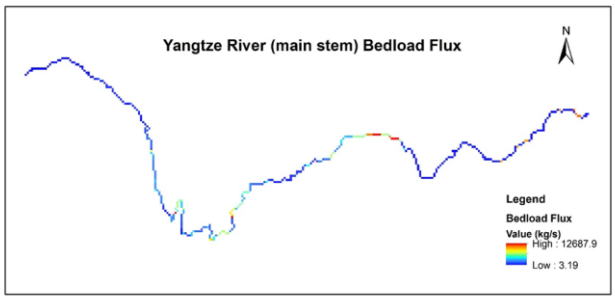

(b)

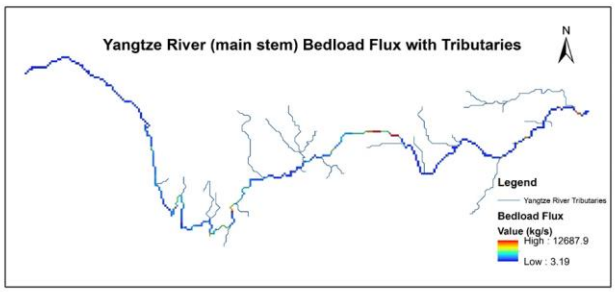

(c)

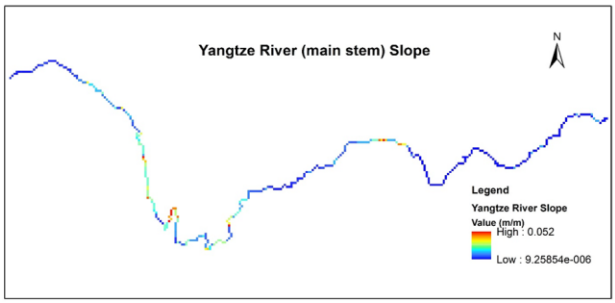

(d)

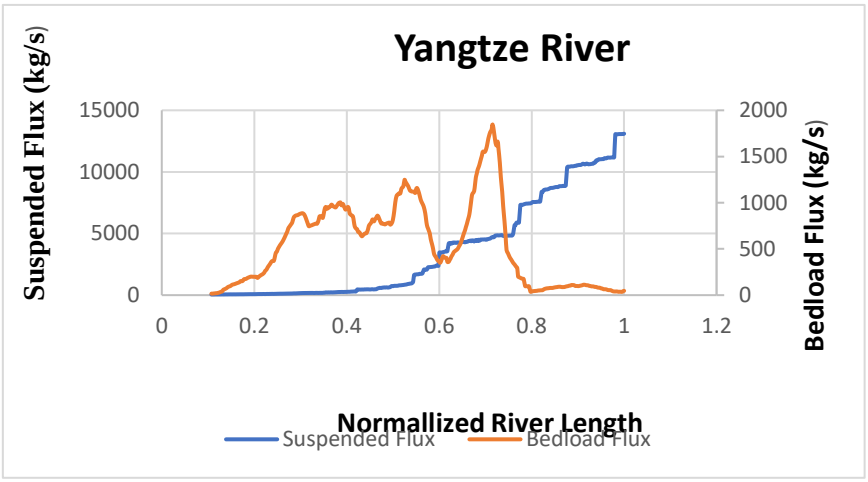

(e)

Figure 23: Longitudinal profile of Yangtze River (In upper row from left to right represent (a) Suspended flux, (b) Bedload flux, in second row from left to right (c) Bedload flux with tributaries, and (d) Slope) and Relationship graph of bedload and suspended flux with normalized stream length in lower row

3.5.3 Ganges River: The Ganges River ranks first with the Brahmaputra for high sediment flux (ref.). The Ganges River originates in the Himalaya Mountains, carries a huge amount of sediment while flowing through the Bengal Basin, and drains to the Bay of Bengal. Due to the annual monsoon, the Ganges basin gets a high amount of rain, which increases discharge as well as sediment transport. **Figure 24 (a) and (b**) shows the longitudinal profile of the Ganges River, and the amount of sediment (both suspended and bedload) transported by the main stem is represented by different colors (dark blue represents low flux and dark red indicates high flux). Normalized stream length (0-1) is represented on the x-axis, suspended flux is represented on the y-axis, and bedload on the secondary y-axis. Lower values on the x-axis (starts from 0) indicate the upstream of the river, and the highest values (up to 1) indicate the downstream of the river. On the secondary y-axis, the moving average of bedload flux is represented in orange, and highly fluctuating bedload fluxes have been smoothed to get a normal trend for better comprehension. Also, the relationship of stream length and sediment flux (both suspended and bedload) is displayed in **Figure 24 (e)**. The longitudinal profile and relationship graph both show increasing trends of suspended flux through the river. Huge suspended flux is shown in the downstream of the river, mainly due to high discharge caused by monsoon rain and the ice-melted water flow from the Himalayas. The overall bedload flux transport is low, comparing to the amount of suspended flux. This is mainly due to the lower relief in the Ganges basin area. An increase in bedload flux is observed at the origin area due to snow-melted water flow, and at an area of confluence in the lower part of the river; other than that bedload seems to have a low continuous trend.

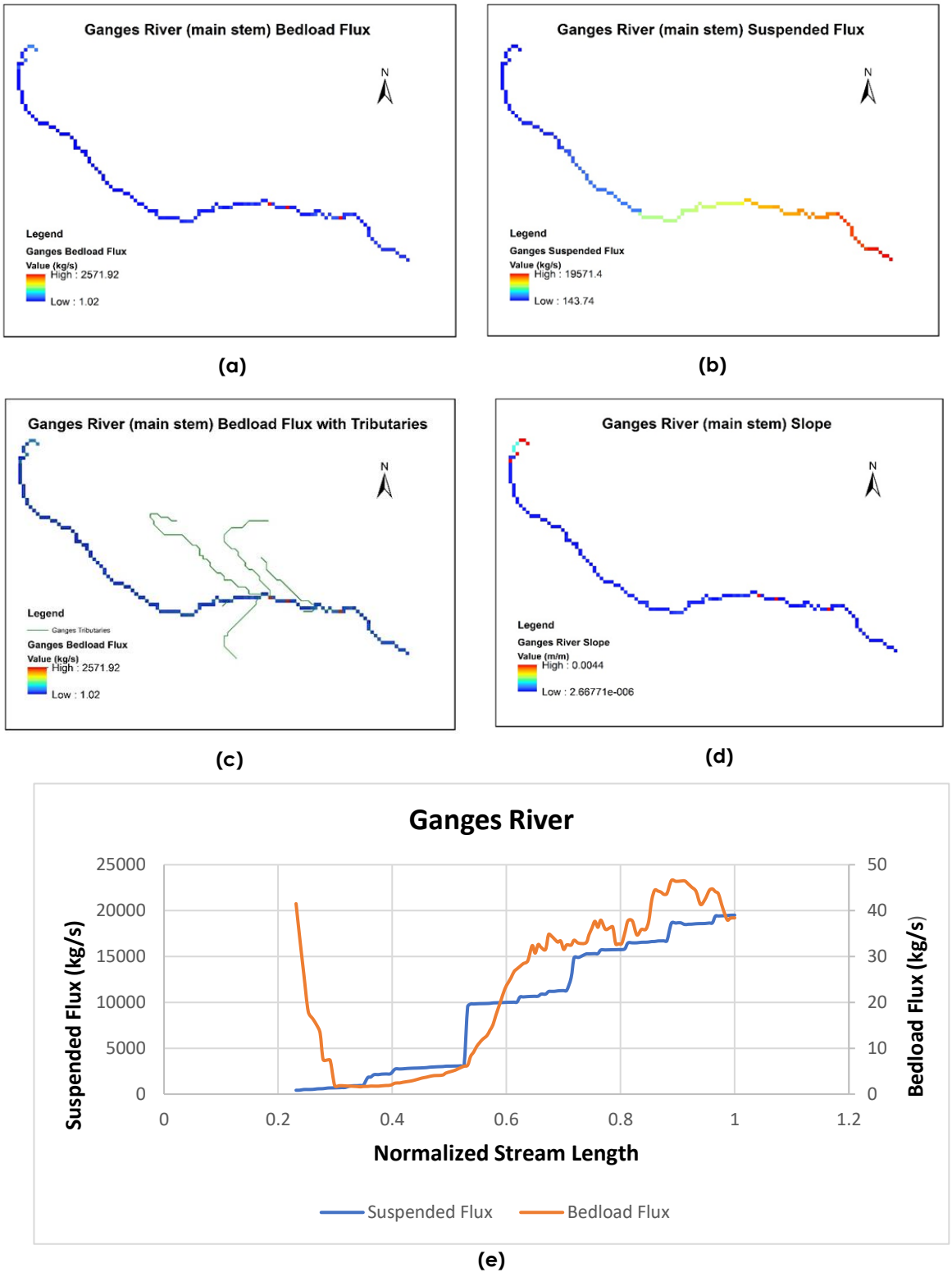

Figure 24: Longitudinal profile of Ganges River (In upper row from left to right represent (a) Suspended flux, (b) Bedload flux, in second row from left to right (c) Bedload flux with tributaries, and (d) Slope, and Relationship graph of bedload and suspended flux with normalized stream length is given in lower row

3.6 Comparison of Bedload Flux and Percentage in Rivers Main Stem

From the bedload flux comparison graph (Figure 25), where normalized stem length is shown in the x-axis (0 representing upstream and 1 downstream) and smoothed (data with high bias has been omitted) log bedload flux of all the rivers (Mississippi, Ganges, and the Yangtze) are presented on the y-axis. Among these three rivers, the Ganges has the lowest bedload flux, showing an increasing downward pattern. The Yangtze shows the highest bedload transport, especially in the mid-stream, because of the high-slope valley run in the middle part of the river. Due to high slopes in these areas, along with high precipitation, this part of the river gets high bedload transport (shown in dark orange in **Figure 25**). The Mississippi also shows a downstream-increasing pattern of bedload flux due to high water inflow from the Missouri and Ohio rivers, along with other tributaries. The Ganges shows an increasing flux in the headwaters due to snow-melt water from the Himalayas, then gradually decreasing until reaching downstream and getting water flow from tributaries.

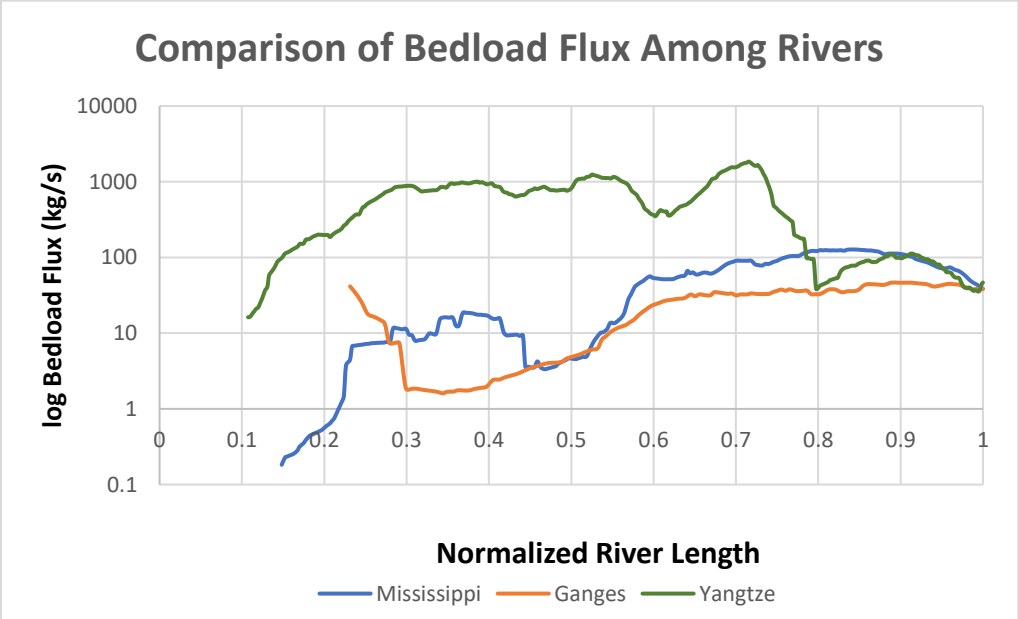

Figure 25: Bedload Flux Comparison Among Large Rivers

Unlike the amount of bedload flux, the percentage of bedload in the total load doesn't show a downstream increasing trend, but rather a downstream decreasing pattern, although bedload flux amount increases downstream as well as suspended sediment. Compared to the increase in suspended sediment, the increasing percentage of bedload is low, which is obvious because bedload needs higher discharge and energy to transport than suspended sediment transport. The overall high percentage is observed in the Yangtze River with an average of 38% (shown in dark green in **Figure 26**) and can reach up to 80%. The Ganges has the lowest average among all, only 0.48% and can be reach up to 8.8 %(shown in orange in figure 27). The Mississippi River has an average of 5.8%, while it can reach up to 25%.

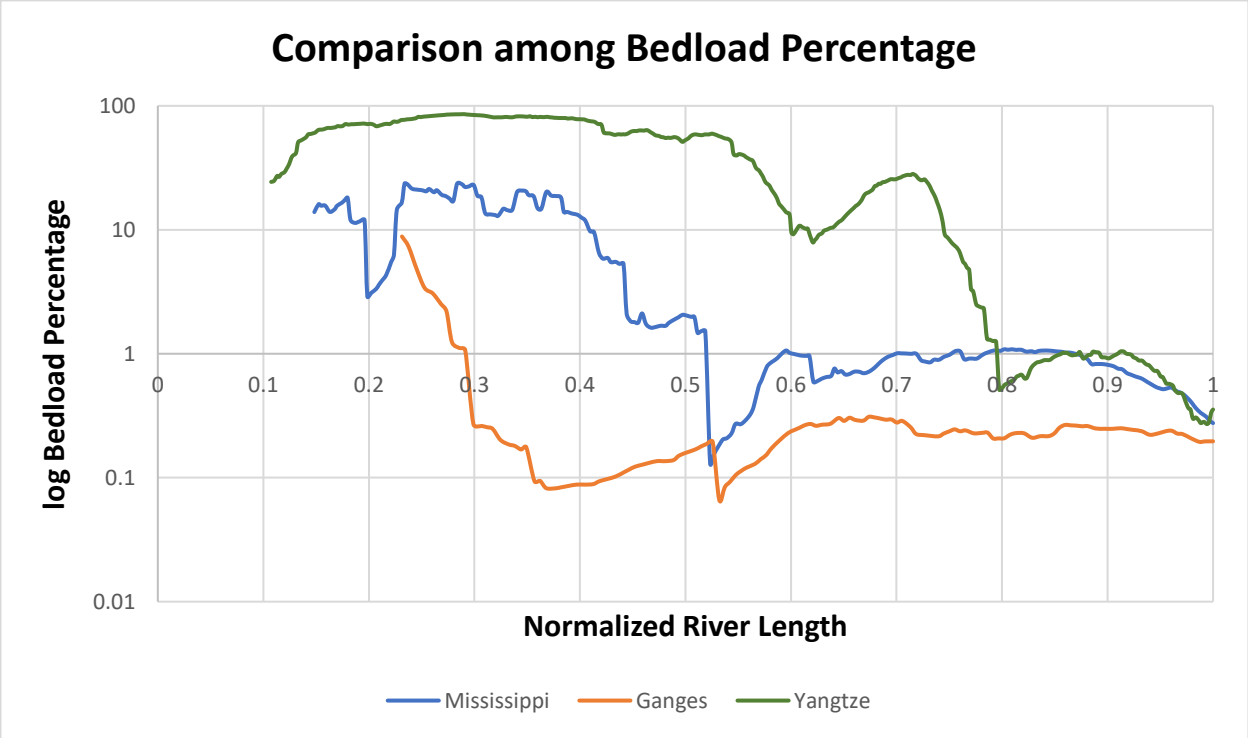

Figure 26: Bedload Flux Percentage Comparison among Rivers

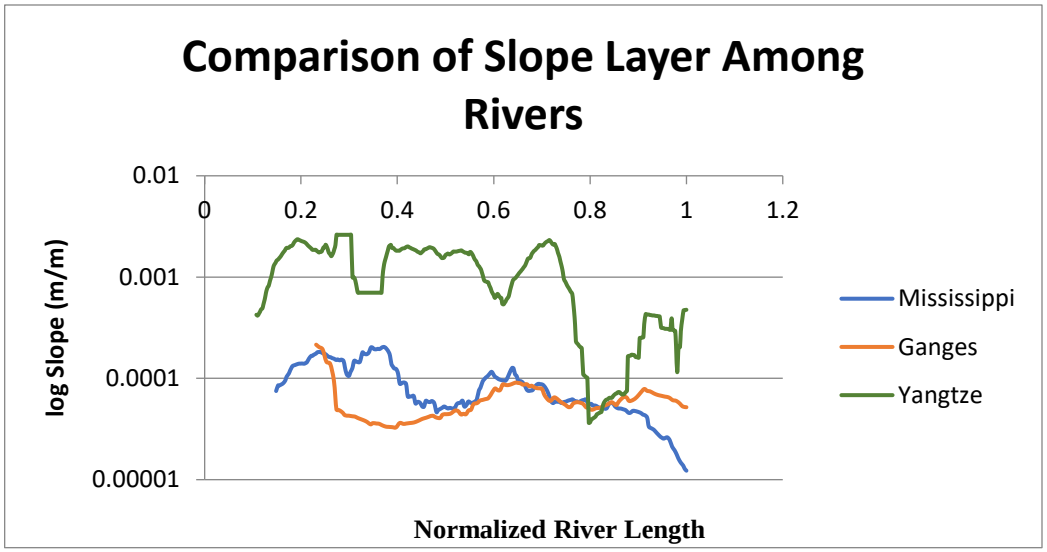

Figure 27: Slope Comparison Among Large Rivers

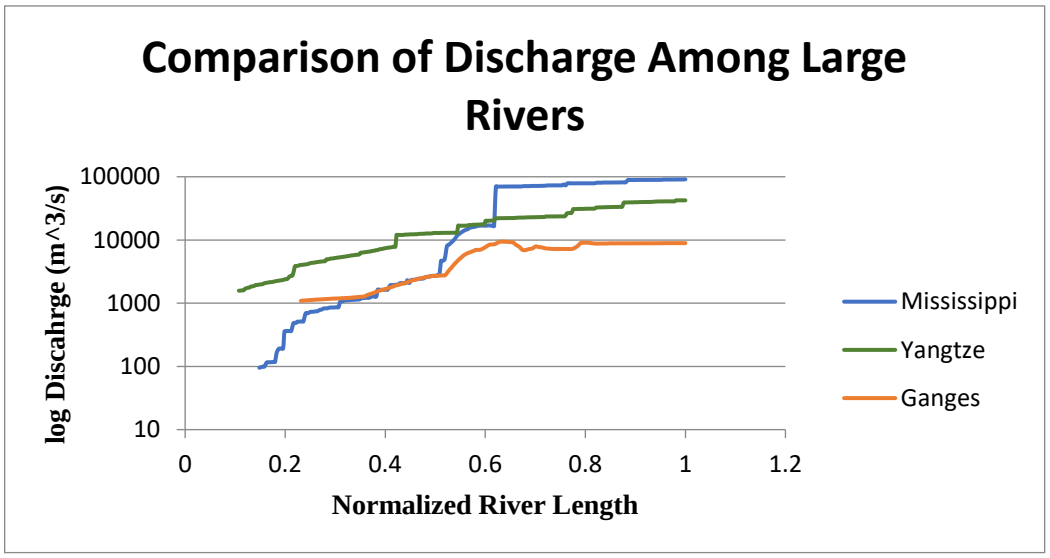

Figure 28: Comparison of Discharge Among Large Rivers

From **Figure 28 and 29,** slope has been found very crucial for shaping the pattern of bedload trend while suspended sediment is mainly found dependency on discharge.

CHAPTER 4

CONCLUSION

Generating a new global bedload dataset (WBMsed-generated) is an attractive pathway for improving the comprehension of large-scale sediment dynamics. Since bedload plays an important role in a variety of geomorphological and hydrological regimes, accurate bedload prediction can help to determine different river and sediment dynamics. A methodology for calculating bedload flux within the global-scale sediment modeling framework (WBMsed) was presented. The resulting dataset of WBMsed can fill the gap of observational deficiency in global rivers, especially for larger rivers.

The bedload flux model result has been validated against observational datasets (collected from secondary sources) for large (>1,000 km^2) rivers. The validation results show that the model only moderately corresponds with observed datasets. The validation result shows that calculated bedload flux overestimates bedload for most of the observed rivers. Considering the high temporal variation within the validation data and lack of continuous data, the results seem promising. Some of the validation data have very few observation points and represent low temporal variation, which decreases validation results. Moreover, considering that the model is run in pristine condition, this first order of estimation can be accepted as viable, because WBMsed is not yet able to incorporate anthropogenic impacts on bedload transport.

A moderate correlation (around R^2=0.45 and 0.50) between observed and modeled discharge and slope leads to the conclusion that, with better discharge prediction, more robust bedload flux prediction capabilities can be achieved. From the analysis of different influential parameters of bedload, only discharge is found as significantly influential on bedload flux, which strengthens the importance of increasing its accuracy within the model.

Manually calculating the model's governing bedload equation showed that river slope is not a strong contributor to the model at this spatial resolution. Using higher-resolution modeling and river slope input may therefore improve the model predictions.

Sediment (both bedload and suspended) dynamics along a few river stems has been investigated for selected rivers. For all the rivers, suspended sediment gradually increased downstream while bedload flux has been found to be more dynamic.

Although the model does not yet provide accurate local bedload prediction, this first-order estimation may be used to gain large-scale insights into large fluvial process. Future developments and applications, based on this study, have the potential for considerably improving the model predictive accuracy.

REFERENCES

Abrahart, R. J. and White, S. M., (2001). Modeling Sediment Transfer in Malawi: Comparing Back Propagation Neural Network Solutions Against a Multiple Linear Regression Benchmark Using Small Data Set, Phys. Chem. Earth Part B 2001, 26 (1).

Almedeij, J. H. and Diplas P. (2003), Bedload transport in gravel-bed streams with unimodal sediment, Journal of Hydraulic Engineering, 129, 896.

Bagnold, R. A., (1966). "An Approach to the Sediment Transport Problem from General Physics," Geological Survey Prof. Paper 422-1, Wash.

Bagnold, R.A., (1980). An empirical correlation of bed load transport rates in flumes and natural rivers. Proceedings of the Royal Society of London. 372, 453–473.

Barry, J.J., Buffington J. M., King J.G., (2004). A general power equation for predicting bed load transport rates in gravel Bed Rivers. Water Resources Research 40.

Barry, J.J., Buffington JM, Goodwin P, King JG, Emmett WW (2008) Performance of bed-load transport equations relative to geomorphic significance: predicting effective discharge and its transport rate. J Hydraul Eng, ASCE 134(5):601–615.

Barry, J.J., Buffington JM, Goodwin P, King JG, Emmett WW (2008) Performance of bed-load transport equations relative to geomorphic significance: predicting effective discharge and its transport rate. J Hydraul Eng, ASCE 134(5):601–615.

Bathurst, J.C., (2007). Effect of coarse surface layer on bed-load transport Journal of Hydraulic Engineering. 133 (11), 1192–1205.

Biemans, H., Haddeland, I., Kabat, P., Ludwig, F., Hutjes, R.W.A., Heinke, J., von Bloh, W., Gerten, D., 2011. Impact of reservoirs on river discharge and irrigation water supply during the 20th century. Water Resour. Res. 47.

Bravo-Espinosa, M., W. Osterkamp, and V. L. Lopes (2003), Bedload transport in alluvial channels, Journal of Hydraulic Engineering, 129, 783.

Chang, Y.L., (1939). Laboratory investigation of flume traction and transportation. Proceedings of the American Society of Civil Engineers. Civil Eng. 104, 1246–1284.

Cohen, S., A. J. Kettner, and J. Syvitski (2014), Global suspended sediment and water discharge dynamics between 1960 and 2010: Continental trends and intra - basin sensitivity, Global Planet. Change, 115, 44–58.

Cohen, S., et al, 2017. Global River Slope: A New Geospatial Dataset and Global-scale Analysis. Under Review.

Cohen, S., Kettner, A.J., Syvitski, J.P.M., Fekete, B.M., (2013). WBMsed, a distributed globalscale riverine sediment flux model: model description and validation. Computers & Geosciences 53, 80–93.

Du Boys, M.P., (1879). The Rhone and streams with movable beds. Annals des Pontes et Chaussees, Tome XVIII.

Einstein, A., (1944). No Title. In Bed-load transportation in mountain creek.

Einstein, H.A., (1950). The bed-load function for sediment transportation in open channel flows, U.S.

Emmett, W. W. (1984), Measurement of bedload in rivers, Erosion and sediment yield: Some methods of Eos. Trans. Amer. Geophys. Union 89 (10), 93–94. Experiments and modeling, J. Geophys. Res., 115, F04001, doi:10.1029/2009JF001628.

Garcia, C., Laronne, J.B., and Sala, M., 2000. Continuous monitoring of bedload flux in a mountain gravel-bed river. Geomorphology, 34, 23–31.

Gilbert, G.K., (1914). The transportation of débris by running water. U.S. Geological Survey Professional Paper 86, 263 pp.

Gomez B (1991) Bedload transport. Earth Sci Rev 31(2):89–132. doi:10.1016/0012-8252(91)90017-A.

Gomez, B. (2006). The potential rate of bed-load transport. Proceedings National Academy of Sciences USA 103(46): 17170–17173.

Gomez, B., and M. Church (1989), An assessment of bed load sediment transport formulae for gravel bed rivers, Water Resources Research, 25(6), 1161-1186.

Graf, W., and M. Altinakar (1996), Hydraulique Fluviale: Écoulement non Permanent et Phénomènes de Transport, Eyrolles, Paris.

Habersack, H.M., Laronne JB (2002) Evaluation and improvement of bed load discharge formulas based on Helley-Smith sampling in an Alpine Gravel Bed River. J Hydraul Eng, ASCE 128(5):484–499.

Habibi, M., Sivakumar M (1994) New formulation for estimation of bed load transport. Paper presented at the International Conference on Hydraulics in Civil Engineering: ‘Hydraulics Working with the Environment’, Brisbane, Australia.

Hamamori, A., (1962). A Theoretical Investigation on the Fluctuations of Bed Load Transport. Report R4, Delft Hydraulics Laboratory, Delft, The Netherlands, 14 pp.

Hinton, D. D. (2012). Complexity of Bed-Load Transport in Gravel Bed Streams: Data Collection, Prediction, and Analysis. All Theses and Dissertations. 3384.

Kabir, M.A., Dutta D, Hironaka S, Peng A (2012) Analysis of bed load equations and river bed level variations using basin-scale process-based modelling approach. Water Resour Manag 26:1143–1163.

Kettner, A. J., & Syvitski, J. P. M. (2008). HydroTrend v.3.0: A climate-driven hydrological transport model that simulates discharge and sediment load leaving a river system. Computers & Geosciences, 34(10), 1170-1183.

Kettner, A.J., Restrepo, J.D., Syvitski, J.P.M., 2010. A spatial simulation experiment to replicate fluvial sediment fluxes within the Magdalena River, Colombia. J. Geol. 118,363–379.

Kettner, A.J., Syvitski, J.P.M., 2009. Fluvial responses to environmental perturbations in the Northern Mediterranean since the Last Glacial Maximum. Quaternary Science Reviews 28 (23–24), 2386–2397.

Khorram, S., Ergil M (2010). Most influential parameters for the bed-load sediment flux equations used in alluvial rivers. J Am Water Resour Assoc 46(6):1065–1090.

King, J.G., Emmett W.W., Whiting P.J., Kenworthy R.P., Barry J.J., (2004). Sediment transport data and related information for selected coarse-bed streams and rivers in Idaho. US Department of Agriculture Forest Service Rocky Mountain Research Station General Technical Report RMRS–GTR–131.

Lajeunesse, E., L. Malverti, and F. Charru (2010), Bed load transport in turbulent flow at the grain scale.

Lechalas, C. (1871), Note sur les rivières à fond de sable, Annales des Ponts et Chaussées, Mémoires et Documents, 5ème série, 1, 381–431.

Leopold, L.B, Emmett WW. (1976). Bedload measurements, East Fork River, Wyoming. Proceedings National Academy of Sciences USA 73(4): 1000–1004.

Leopold, L.B, Emmett WW. (1997). Bedload and river hydraulics–inferences from the East Fork River, Wyoming. US Geological Survey Professional Paper 1583.

Liu, Y., F. Metivier, E. Lajeunesse, P. Lancien, C. Narteau, and P. Meunier (2008), Measuring bed load in gravel bed mountain rivers: Averaging methods and sampling strategies, Geodin. Acta, 21, 81–92.

Martin, Y., (2003). Evaluation of bedload transport formula using field evidence from the Vedder River, British Columbia. Geomorphology, 53(1), 75-95.

Meade, R.H., Yuzyk, T.R., and Day, T.J., (1990), Movement and storage of sediment in rivers of the United States and Canada, in Wolman, M.G., and Riggs, H.C., eds., Surface water

hydrology—The geology of North America: Boulder, Colo., Geological Society of America, p. 255–280.

Métivier, F., P. Meunier, M. Moreira, A. Crave, C. Chaduteau, B. Ye, and G. Liu (2004), Transport dynamics and morphology of a high mountain stream during the peak flow season: The Ürümqi River (Chinese Tian Shan), in River Flow 2004, vol. 1, pp. 770–777, A. A. Balkema, Leiden, Netherlands.

Meunier, P., F. Metivier, E. Lajeunesse, A. S. Meriaux, and J. Faure (2006), Flow pattern and sediment transport in a braided river: The "torrent de St Pierre" (French Alps), J. Hydrol., 330, 496–505.

Meunier, P., F. Metivier, E. Lajeunesse, A. S. Meriaux, and J. Faure (2006), Flow pattern and sediment transport in a braided river: The "torrent de St Pierre" (French Alps), J. Hydrol., 330, 496–505.

Meyer-Peter, E., Müller, R. (1948) Formulas for bed-load transport. Paper presented at the 2nd Meeting of the International Association of Hydraulic Structures Research, Madrid.

Milliman, J.D., Meade, R.H., 1983. World-wide delivery of river sediment to the oceans. J. Geol. 91 (1), 1–21.

Milliman, J.D., Syvitski, J.P.M., 1992. Geomorphic/tectonic control of sediment discharge to the ocean— the importance of small mountainous rivers. Journal of Geology 100 (5), 525–544.

Mueller, E.R., Pitlick, J., Nelson, J.M. (2005) Variation in the reference Shields stress for bed load transport in gravel-bed streams and rivers. Water Resour Res 41(4):W04006.

Nittrouer, J.A., Allison, M.A. & Campanella, R., (2008). Bedform transport rates for the lowermost Mississippi River. Journal of Geophysical Research: Earth Surface, 113(3), pp.1–16.

Paola, C., (1996). Incoherent Structure: Turbulence as a Metaphor for Stream Braiding, in Coherent Flow Structures in Open Channels (Eds.: P. J. Ashworth, S. J. Bennett, J. L. Best, S. J. McLelland), John Wiley and Sons, Hoboken, NJ, pp. 705–723.

Parker, G. (1990), Surface-based bedload transport relation for gravel rivers, Journal of Hydraulic Research JHYRAF, 28(4).

Parker, G., and P. C. Klingeman (1982), On why gravel bed streams are paved, Water Resources Research, 18(5), 1409-1423.

Parker, G., Klingeman, P.C., McLean, D.G., (1982). Bedload and the size distribution of paved gravel-bed streams. Journal of the Hydraulics Division. 108 (4), 544–571.

Raven, E. K., Lane, S.N., Ferguson, R.I., (2010). Using Sediment Impact Sensors to Improve the Morphological Sediment Budget Approach Estimating Bed Load Transport Rates, Geomorphology 2010, 119, 125–134.

Reid, I., Powell, D.M., and Laronne, J.B., (1996). Prediction of bedload transport by desert flash floods. Journal of Hydraulic Engineering, 122(3), 170-173.

Rickenmann, D., Turowski, J.M., Fritschi, B., Klaiber, A., Ludwig, A. (2012). Bedload transport measurements at the Erlenbach stream with geophones and automated basket samplers. Earth Surface Processes and Landforms, 37(9):1000–1011.

Rottner, J., (1959). A formula for bed load transportation. La Houille Blanche 3 (4), 301–307.

Ryan, S.E., Emmett WW., (2002). The nature of flow and sediment movement in Little Granite Creek near Bondurant, Wyoming. US Department of Agriculture Forest Service Rocky Mountain Research Station General Technical Report RMRS–GTR–90.

Schoklitsch, A., (1950). Handbuch des wasserbaues. Springer, New York.

Shields, A., (1936). Anwendung der Aehnlichkeitsmechanik und der Turbulenzforschung auf die Geschiebebewegung, Mitteilungen der Preussischen Versuchsanstalt für Wasserbau und Schiffbau, Berlin, 26 pp.

Sinnakaudan, S., Ab A.S. Ghani, M.S. Ahmad, and N.A. Zakaria, (2006). Multiple Linear Regression Model for Total Bed Material Load Prediction. Journal of Hydraulic Engineering, ASCE 132(5):521-528.

Syvitski, J. P. M., & Saito, Y. (2007). Morphodynamics of deltas under the influence of humans. Global and Planetary Change, 57(3-4), 261–282.

Syvitski, J. P. M., & Saito, Y. (2007). Morphodynamics of deltas under the influence of humans. Global and Planetary Change, 57(3-4), 261–282.

Syvitski, J.P.M., Kettner, A.J., Peckham, S.D., Kao, S.J., 2005. Predicting the flux of sediment to the coastal zone: application to the Lanyang watershed, Northern Taiwan. J. Coast. Res. 21, 580–587.

Syvitski, J.P.M., Milliman, J.D., (2007). Geology, geography, and human's battle for dominance over the delivery of fluvial sediment to the Coastal Ocean. The Journal of Geology, 115, 1–19.

Syvitski, J.P.M., Milliman, J.D., 2007. Geology, geography, and humans battle for dominance over the delivery of fluvial sediment to the coastal ocean. J. Geol. 115 (1), 1–19.

Syvitski, J.P.M., Vorosmarty, C.J., Kettner, A.J., Green, P., 2005. Impact of humans on the flux of terrestrial sediment to the global coastal ocean. Science 308 (5720), 376–380.

Thaxton C., (2004). Investigations of grain size dependent sediment transport phenomena on multiple scales. PhD dissertation. North Carolina State University, Raleigh, NC.

Turowski, J.M., Rickenmann, D., Dadson, S.J., (2010). The partitioning of the total sediment load of a river into suspended load and bedload: A review of empirical data. Sedimentology, 57, 1126–1146.

USWES, (1935). Study of River-Bed Material and Their Use with Special Reference to the Lower Mississippi River. United States Waterways Experiment Station, Vicksburg, MS, Paper 17, 16pp.

Vörösmarty, C.J., Federer, C.A., Schloss, A.L., 1998. Potential evaporation functions compared on US watersheds: possible implications for global-scale water balance and terrestrial ecosystem modeling. Journal of Hydrology 207, 147–169.

Vörösmarty, C.J., Fekete, B.M., Meybeck, M., Lammers, R.B., 2000. Geomorphometric attributes of the global system of rivers at 30-minute spatial resolution. J. Hydrol. 237 (1–2), 17–39.

Vörösmarty, C.J., Meybeck, M., Fekete, B., Sharma, K., 1997. The potential of neo-Castorization on sediment transport by the global network of rivers Human impact on erosion and sedimentation. IAHS 245, 261–273.

Vörösmarty, C.J., Moore III, B., Grace, A.L., Gildea, M., Melillo, J.M., Peterson, B.J., Rastetter, E.B., Steudler, P.A., 1989. Continental scale models of water balance and fluvial transport: an application to South America. Global Biochemical Cycles 3, 241–265.

Vörösmarty, C.J., Sharma, K.P., Fekete, B.M., Copeland, A.H., Holden, J., Marble, J., Lough, J.A., 1997b. The storage and aging of continental runoff in large reservoir systems of the world. Ambio 26, 210–219.

Walling, D. E. & Fang, X. (2003) Recent trends in the suspended sediment loads of the world's rivers. Global & Planetary Change 39, 111–126.

Wang, X., Yang Q, Lu W, Wang X (2011) Effects of bed load movement on mean flow characteristics in mobile gravel beds. Water Resour Manag, Online First™, 10 June 2011.

Whipple, K.X., (2004). Bedload Rivers and the geomorphology of active orogens. Annu. Rev. Earth Planet Sci., 32, 151-185.

Wilcock, P. R. (2001), Toward a practical method for estimating sediment transport rates in gravel bed rivers, Earth Surface Processes and Landforms, 26(13), 1395-1408.

Wisser, D., Fekete, B.M., Vörösmarty, C.J., Schumann, A.H., 2010a. Reconstructing 20th century global hydrography: a contribution to the Global Terrestrial Network–Hydrology (GTN–H). Hydrology and Earth System Sciences 14 (1), 1–24.

Wisser, D., Fekete, B.M., Vörösmarty, C.J., Schumann, A.H., 2010. Reconstructing 20th century global hydrography: a contribution to the Global Terrestrial Network-Hydrology (GTN-H). Hydrol. Earth Syst. Sci. 14 (1), 1–24.

Wollheim,W.M., Vörösmarty, C.J., Bouwman, A.F., Green, P., Harrison, J., Linder, E., Peterson, B.J., Seitzinger, S.P., Syvitski, J.P.M., 2008. Global N removal by freshwater aquatic systems using a spatially distributed, within-basin approach. Glob. Biogeochem. Cycles 22.

Zhang, X. and G.L. McConnachie, (1994). A Reappraisal of the Engelund Bed-Load Equation. Journal of Hydrological Science 39(6):561-567.